The improvement rate on laboratory examinations was significantly greater for treatments including PE (PE and PE+IVIG/CS groups) than for those without PE (CS and IVIG groups) (8/14, 57.1% vs. 2/16, 12.5%, p=0.0187).

3.3.4. Effects of treatments on blood tests

Changes in hematological examinations are summarized in Table 5. Overall, the percentage of eosinophils fell significantly from 5.04 to 2.85 (p=0.049), and among the immunotherapies, reduction was significant only in treatments with CS. The total and allergen-specific IgEs did not change significantly.

4. Discussion

In the present study, we have disclosed for the first time the responses of atopic myelitis to various immunotherapies. In our series, three-quarters of patients with atopic myelitis responded, more or less, to immunotherapies; indicating that spinal cord dysfunction in this condition is partly reversible, although most of the patients showed a persistent clinical course. Interestingly, PE with or without IVIG/CS was found to be significantly superior to CS and IVIG alone by laboratory tests and the improvement rates in neurological findings were also higher in the former. The retrospective nature of the study as well as the relatively small number of treatments limit the significance of the results, however, laboratory studies such as spinal cord MRI and evoked potentials supplemented the neurological evaluation.

Atopic myelitis frequently presents a chronic persistent course, and the MRI lesions do not change in size over years masquerading as spinal cord tumors [1–3,7,9,10]. Thus, in the present series, immunotherapy was initiated months or years after the onset. Nevertheless, neurological signs and the EDSS scores were improved in three-quarters and one-third of the patients, respectively. Moreover, half the patients showed improvement on either MRI or by EPs. These findings suggest the inflammatory nature of spinal cord lesions, partly reversible by immunotherapy, despite the persistence of small MRI lesions and normal CSF findings [1–3,7]. The notion is consistent with the neuropathological observations indicating chronic active inflammation [9,10].

Concerning the modality of the immunotherapies, PE and PE+IVIG/CS were the most favorable, as determined by neurological examination and laboratory tests, while IVIG was the least effective and CS showed a modest improvement rate as determined by laboratory tests. Although the disease duration at the time of treatment was longer and the EDSS scores were greater in the PE+IVIG/CS group than in the other groups, the treatment was more efficacious than CS and IVIG on laboratory tests.

The high efficacy of PE suggests that humoral factors, possibly driven by Th2 cells, may contribute to sustaining inflammation in the spinal cord. CS treatment was also effective on neurological examination. Its efficacy is similar in other atopic disorders such as bronchial asthma, atopic dermatitis and allergic rhinitis [16–18]; which may be partly attributable to the significant decrease in eosinophils, since they have been shown to infiltrate the spinal cord lesions and their activated products are deposited in the tissues [9,10]. Although the number of trials was small in the IVIG group, its ineffectiveness may suggest that an autoantibody-mediated mechanism does not play a major role in this condition.

Both pathological studies showing eosinophil infiltration and axonal damage from the early course of the disease, and flow cytometric studies on the cytokine balance in peripheral blood lymphocytes showing Th2 dominance in atopic myelitis versus Th1 dominance in MS, indicate that distinct mechanisms are operative between these two conditions [19–22]. In autoimmune diseases affecting the central nervous system (CNS), such as MS, CS has been shown to be effective in an acute phase to reduce the inflammatory response and shorten the exacerbating phase [23]. In contrast, CS appeared to be less effective than PE for atopic myelitis, as shown in the representative case in Fig. 2, further supporting the notion that a distinctive mechanism is operative in this condition. The efficacy of PE appears to be similar to that reported for atypical demyelinating diseases, such as Devic disease [24], in which eosinophils and a Th2-driven mechanism have also been suggested to play roles [25]. PE may be effective for removing activated eosinophil products, such as eosinophil cationic protein (ECP) and major basic protein, which have been shown to be deposited in the spinal cord lesions in atopic myelitis patients [9,10]. Alternatively, removal of cytokines, complements or immune complexes may be relevant.

In summary, our results suggest that immunotherapies, especially those including PE, may be worth trying, even in cases showing a protracted clinical course, long after the onset of myelitis with atopic diathesis. Further studies focusing on cytokines and eosinophil products in the CSF before and after immunotherapy will be required to clarify the mechanism of action.

Acknowledgements

This work was supported in part by a Neuroimmunological Disease Research Committee grant, a Research on Brain Science grant from the Ministry of Health and Welfare, Japan, and Grants 12470142, 12557060 and 12877097 from the Ministry of Education, Science, Sports and Culture, Japan.

References

[1] Kira J, Yamasaki K, Kawano Y, Kobayashi T. Acute myelitis associated with hyperIgEemia and atopic dermatitis. J Neurol Sci 1997;148:199–203.

[2] Kira J, Kawano Y, Yamasaki K, Tobimatsu S. Acute myelitis with hyperIgEaemia and mite antigen specific IgE: atopic myelitis. J Neurol Neurosurg Psychiatry 1998;64:676–9.

[3] Kira J, Kawano Y, Horiuchi I, Yamada T, Imayama S, Furue M, et al. Clinical, immunological and MRI features of myelitis with atopic dermatitis (atopic myelitis). J Neurol Sci 1999;162:56–61.
[4] Horinouchi H, Inobe J, Mori T, Kumamoto T, Tsuda T. A case of atopic myelitis. Rinsho Shinkeigaku 2000;40:218–21.
[5] Furuya T, Miwa H, Hatano T, Miyashita N, Tanaka S, Mizuno Y. Clinical features of myelitis in patients with atopic symptoms. No To Shinkei 2001;53:241–5.
[6] Kuwabara T, Tanaka M. A case of atopic myelitis in the area other than Kyushu Island. Rinsho Shinkeigaku 2001;41:621–4.
[7] Osoegawa M, Ochi H, Minohara M, Murai H, Umehara F, Furuya H, et al. Myelitis with atopic diathesis: a nationwide survey of 79 cases in Japan. J Neurol Sci 2003;209:5–11.
[8] Mosmann TR, Sad S. The expanding universe of T-cell subsets: Th1, Th2 and more. Immunol Today 1996;17:138–46.
[9] Kikuchi H, Osoegawa M, Ochi H, Murai H, Horiuchi I, Takahashi H, et al. Spinal cord lesions of myelitis with hyperIgEemia and mite antigen specific IgE (atopic myelitis) manifest eosinophilic inflammation. J Neurol Sci 2001;183:73–8.
[10] Osoegawa M, Ochi H, Kikuchi H, Shirabe S, Nagashima T, Tsumoto T, et al. Eosinophilic myelitis associated with atopic diathesis: a combined neuroimaging and histopathological study. Acta Neuropathol (Berl) 2003;105:289–95.
[11] Rothe MJ, Grant-Kels JM. Atopic dermatitis: an update. J Am Acad Dermatol 1996;35:1–13 [quiz 4–6].
[12] McDonald WI, Compston A, Edan G, Goodkin D, Hartung HP, Lublin FD, et al. Recommended diagnostic criteria for multiple sclerosis: guidelines from the International Panel on the diagnosis of multiple sclerosis. Ann Neurol 2001;50:121–7.
[13] Kurtzke JF. Rating neurologic impairment in multiple sclerosis: an expanded disability status scale (EDSS). Neurology 1983;33: 1444–52.
[14] Sipe JC, Knobler RL, Braheny SL, Rice GP, Panitch HS, Oldstone MB. A neurologic rating scale (NRS) for use in multiple sclerosis. Neurology 1984;34:1368–72.
[15] Suga R, Tobimatsu S, Kira J, Kato M. Motor and somatosensory evoked potential findings in HTLV-I associated myelopathy. J Neurol Sci 1999;167:102–6.
[16] Rudikoff D, Lebwohl M. Atopic dermatitis. Lancet 1998;351: 1715–21.
[17] Nielsen LP, Dahl R. Comparison of intranasal corticosteroids and antihistamines in allergic rhinitis: a review of randomized, controlled trials. Am J Respir Medicine 2003;2:55–65.
[18] Leone FT, Fish JE, Szefler SJ, West SL. Systematic review of the evidence regarding potential complications of inhaled corticosteroid use in asthma: collaboration of American College of Chest Physicians, American Academy of Allergy, Asthma, and Immunology, and American College of Allergy, Asthma, and Immunology. Chest 2003;124:2329–40.
[19] Horiuchi I, Kawano Y, Yamasaki K, Minohara M, Furue M, Taniwaki T, et al. Th1 dominance in HAM/TSP and the optico-spinal form of multiple sclerosis versus Th2 dominance in mite antigen-specific IgE myelitis. J Neurol Sci 2000;172:17–24.
[20] Wu XM, Osoegawa M, Yamasaki K, Kawano Y, Ochi H, Horiuchi I, et al. Flow cytometric differentiation of Asian and Western types of multiple sclerosis, HTLV-1-associated myelopathy/tropical spastic paraparesis (HAM/TSP) and hyperIgEaemic myelitis by analyses of memory CD4 positive T cell subsets and NK cell subsets. J Neurol Sci 2000;177:24–31.
[21] Ochi H, Wu XM, Osoegawa M, Horiuchi I, Minohara M, Murai H, et al. Tc1/Tc2 and Th1/Th2 balance in Asian and Western types of multiple sclerosis, HTLV-I-associated myelopathy/tropical spastic paraparesis and hyperIgEaemic myelitis. J Neuroimmunol 2001; 119:297–305.
[22] Ochi H, Osoegawa M, Murai H, Minohara M, Taniwaki T, Kira J. Presence of IgE antibodies to bacterial superantigens and increased IL-13-producing T cells in myelitic patients with atopic diathesis. Int Arch Allergy Immunol 2004;134:41–8.
[23] Durelli L, Cocito D, Riccio A, Barile C, Bergamasco B, Baggio GF, et al. High-dose intravenous methylprednisolone in the treatment of multiple sclerosis: clinical-immunologic correlations. Neurology 1986;36:238–43.
[24] Weinshenker BG, O'Brien PC, Petterson TM, Noseworthy JH, Lucchinetti CF, Dodick DW, et al. A randomized trial of plasma exchange in acute central nervous system inflammatory demyelinating disease. Ann Neurol 1999;46:878–86.
[25] Lucchinetti CF, Mandler RN, McGavern D, Bruck W, Gleich G, Ransohoff RM, et al. A role for humoral mechanisms in the pathogenesis of Devic's neuromyelitis optica. Brain 2002;125: 1450–61.

Enhanced Priming of Antigen-Specific CTLs In Vivo by Embryonic Stem Cell-Derived Dendritic Cells Expressing Chemokine Along with Antigenic Protein: Application to Antitumor Vaccination[1]

Hidetake Matsuyoshi, Satoru Senju, Shinya Hirata, Yoshihiro Yoshitake, Yasushi Uemura, and Yasuharu Nishimura[2]

Dendritic cell (DC)-based immunotherapy is regarded as a promising means for anti-cancer therapy. The efficiency of T cell-priming in vivo by transferred DCs should depend on their encounter with T cells. In the present study, we attempted to improve the capacity of DCs to prime T cells in vivo by genetic modification to express chemokine with a T cell-attracting property. For genetic modification of DCs, we used a recently established method to generate DCs from mouse embryonic stem cells. We generated double-transfectant DCs expressing a chemokine along with a model Ag (OVA) by sequential transfection of embryonic stem cells, and then induced differentiation to DCs. We comparatively evaluated the effect of three kinds of chemokines; secondary lymphoid tissue chemokine (SLC), monokine induced by IFN-γ (Mig), and lymphotactin (Lptn). All three types of double transfectant DCs primed OVA-specific CTLs in vivo more efficiently than did DCs expressing only OVA, and the coexpression of SLC or Lptn was more effective than that of Mig. Immunization with DCs expressing OVA plus SLC or Mig provided protection from OVA-expressing tumor cells more potently than did immunization with OVA alone, and SLC was more effective than Mig. In contrast, coexpression of Lptn gave no additive effect on protection from the tumor. Collectively, among the three chemokines, expression of SLC was the most effective in enhancing antitumor immunity by transferred DCs in vivo. The findings provide useful information for the development of a potent DC-based cellular immunotherapy. *The Journal of Immunology,* **2004, 172: 776–786.**

Dendritic cells (DCs)[3] are potent immunostimulators. In vivo transfer of Ag-bearing DCs has proven efficient in priming T cell responses specific to Ag. DC-based methods are now regarded as being a promising approach for immunotherapy, especially for anti-cancer immunotherapy. DCs pulsed with peptide Ags or genetically modified to present Ags are currently being clinically tested in cases of immunotherapy for subjects with malignant tumors (1–4).

The efficiency of T cell-priming in vivo by injected DCs should depend on their encounter with T cells. When exogenous Ag was injected intracutaneously, ~25% of the DCs capturing the Ag migrated to the T cell area of draining lymph nodes (LN) (5), where they presented Ag to prime naive T cells specific to the Ag. In contrast, when bone marrow cell-derived DCs (BM-DCs) or splenic DCs are transferred exogenously by s.c. or i.p. injection, the absolute number of the DCs found within the draining LN represented only a small proportion (0.1–1%) (6–8). It has also been reported that almost all of transferred DCs remained at the s.c. immunization site 24 h after transfer (9). Inefficient migration of exogenous DCs to lymphoid organs may lower the frequency of their encounter with T cells. Therefore, it may be possible to improve the efficacy of exogenously transferred DCs to prime immune responses by augmenting their encounter with T cells. For example, if transferred DCs produce chemokines to intensively attract T cells, they may prime immune response efficiently, even though the DCs do not migrate to lymphoid organs.

Several kinds of chemokines with the capacity to attract T cells are produced by different cell types. Secondary lymphoid tissue chemokine (SLC)/CCL21 is produced in T cell regions of LN and spleen and also by high endothelial venules in LN. SLC chemoattracts T cells, NK cells, B cells, and DCs (10–12). Monokine induced by IFN-γ (Mig)/CXCL9 is produced by macrophages and binds to the chemokine receptor CXCR3, which mediates the recruitment of predominantly Th1 cells and activated NK cells (13). Lymphotactin (Lptn)/XCL1, produced by activated T cells, has chemoattractive properties on $CD4^+$ and $CD8^+$ T cells and on NK cells (14, 15). This chemotactic action of Lptn is mediated through the receptor XCR1.

Recently, we established a novel method for genetic modification of DCs, where we generated DCs from mouse embryonic stem (ES) cells by in vitro differentiation (16). ES cell-derived DCs (ES-DCs) express MHC class II, CD11c, CD80, and CD86. They can strongly simulate MLR and efficiently process and present protein Ag to T cells. Their capacity to do so is comparable to that of BM-DCs. We can readily generate genetically modified DCs by introducing expression vectors driven by a β-actin promoter and subsequent

Department of Immunogenetics, Graduate School of Medical Sciences, Kumamoto University, Kumamoto, Japan

Received for publication April 29, 2003. Accepted for publication September 30, 2003.

The costs of publication of this article were defrayed in part by the payment of page charges. This article must therefore be hereby marked *advertisement* in accordance with 18 U.S.C. Section 1734 solely to indicate this fact.

[1] This work was supported in part by Grants-in-Aid 14657082, 14570421, 14370115, and 12213111 from the Ministry of Education, Science, Technology, Sports, and Culture, Japan, and a research grant for Intractable Diseases from the Ministry of Health and Welfare, Japan.

[2] Address correspondence and reprint requests to Dr. Yasuharu Nishimura, Department of Immunogenetics, Graduate School of Medical Sciences, Kumamoto University, Honjo 1-1-1, Kumamoto 860-8556, Japan. E-mail address: mxnishim@gpo.kumamoto-u.ac.jp

[3] Abbreviations used in this paper: DC, dendritic cell; ES, embryonic stem cell; SLC, secondary lymphoid tissue chemokine; Mig, monokine induced by IFN-γ; Lptn, lymphotactin; LN, lymph node; BM-DC, bone marrow cell-derived DC; ES-DC, ES cell-derived DC; neo-R, neomycin resistant; IRES, internal ribosomal entry site.

0022-1767/04/$02.00

and used as effector cells in cytotoxicity assay using peptide-pulsed EL-4 cells as target cells, as described (16).

Induction of OVA-specific CTLs in vivo

Genetically modified ES-DCs, viable or heat-killed, or OVA protein (50 μg) were injected i.p. to mice twice at 7-day intervals, and 7 days after the second transfer, the mice were killed and spleen cells were isolated. Whole spleen cells were cultured in vitro in the presence of OVA peptide (0.1 μM) for 5 days and OVA-specific CTL activity was analyzed as described (16).

Tumor prevention experiments

In tumor prevention experiments and survival studies, 2×10^4 or 3×10^3 genetically modified ES-DCs were transferred i.p. into mice. Transfers were done twice at 7-day intervals, and 7 days after the second transfer, MO4 cells were challenged s.c. in the shaved left flank region. Tumor sizes were determined biweekly in a blinded fashion and survival rate was monitored. Tumor index was calculated as: Tumor index (in millimeters) = square root (length $\times$ width).

In vivo depletion of $CD4^+$ and $CD8^+$ T lymphocytes

Mice were transferred i.p. twice with 3×10^3 ES-DC-OVA/mock or ES-DC-OVA/SLC at 7-day intervals, and 7 days after the second transfer, the mice were challenged s.c. with 3×10^6 MO4 cells (day 0). The mice were given a total of six i.p. transfers (days -18, -15, -11, -8, -4, -1) of the ascites (0.1 ml/mouse/transfer) from hybridoma-bearing nude mice. mAbs used were rat anti-mouse CD4 (clone GK1.5) and rat anti-mouse CD8 (clone 2.43). Normal rat IgG (Sigma-Aldrich, St. Louis, MO; 200 μg/mouse/transfer) was used as control. Tumor measurements were made 15 days after tumor challenge. Results are expressed as tumor index + SD. Each group included eight mice. Depletion of T cell subsets by treatment with mAbs was confirmed by flow cytometric analysis of spleen cells, which showed a >90% specific depletion.

Histological analysis of tumor tissues

Freshly excised tumor tissues were immediately frozen and embedded in Tissue-Tek OCT compound (Miles, Elkhart, IN). Serial 5-μm sections were made using cryostat and underwent immunochemical staining with mAbs specific to CD4 (L3T4; BD PharMingen, San Diego, CA) or CD8 (Ly-2; BD PharMingen) and N-Histofine Simple Stain Mouse MAX PO (Nichirei, Tokyo, Japan).

Statistical analysis

Two-tailed Student's t test was used to determine the statistical significance of differences in lytic activity of spleen cell preparations and tumor growth, and between treatment groups. A value of $p < 0.05$ was considered significant. The Kaplan-Meier plot for survivals was assessed for significance using the Breslow-Gehan-Wilcoxon test. Statistical analyses were made using StatView 5.0 software (Abacus Concepts, Calabasas, CA).

Results

Profile of chemokine gene expression in ES-DCs

We recently established a culture method to generate DCs from mouse ES cells. ES-DCs have the capacity to stimulate T cells comparable to BM-DCs (16). At the beginning of the present study, to determine the profile of chemokine gene expression by ES-DCs, we analyzed chemokine mRNAs by cDNA macroarray hybridization analysis, comparing ES-DCs and BM-DCs. The gene expression of DC-derived chemokines and chemokines that chemoattract T cells is shown in Fig. 1. The analysis revealed that chemokine gene expression profile of ES-DCs was somewhat different from that of BM-DCs. However, both DCs expressed C10, and expression of T cell-attracting chemokines produced by cells other than DCs such as SLC, Lptn, Mig, or stromal cell-derived factor 1α were rarely detected in both types of DCs generated in vitro. Therefore, we presumed augmentation of the immunomodulating capacity by in vivo transferred DCs through genetic modification of DCs to express such T cell-attracting chemokines.

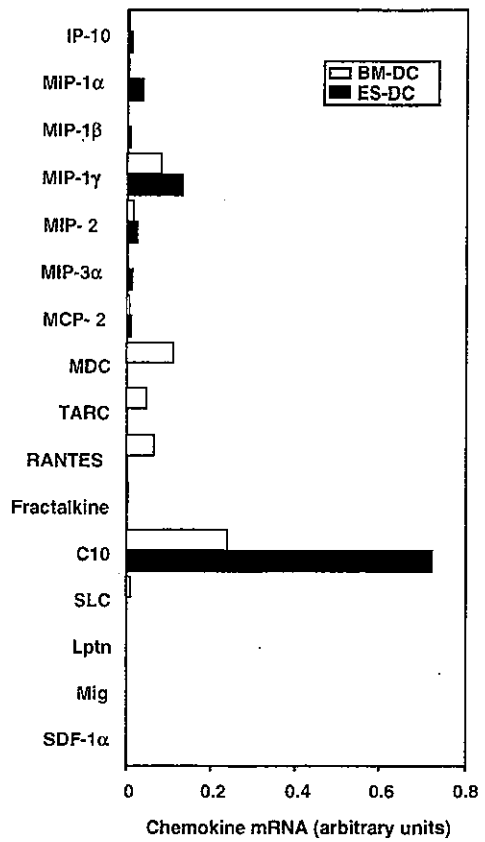

FIGURE 1. Profile of chemokine gene expression in ES-DCs and BM-DCs. Radiolabeled cDNA generated from ES-DCs and BM-DCs were hybridized to chemokine gene-specific 44 cDNA fragments spotted on nylon membranes. The hybridization signals were normalized to the signal derived from β-actin on the same membrane. Data for DC-derived chemokines and chemokines with T cell-attracting property are shown.

Generation of ES-DCs expressing chemokine along with antigenic protein

Using the expression vector driven by the β-actin promoter and containing the IRES-drug-resistant marker gene (Fig. 2, *A* and *B*), we can generate ES cell transfectant clones expressing the gene products after their differentiation to DCs. Using this system, we first prepared an ES cell transfectant clone highly expressing OVA after differentiation to DCs. Subsequently, we introduced chemokine expression vectors or mock vector into the ES cell clone expressing OVA (ES-OVA) (Fig. 2*C*). We selected one double-transfectant ES cell clone for each chemokine gene or mock vector transfection and generated four kinds of ES-DCs expressing chemokine along with OVA or OVA alone, and designated them ES-DC-OVA/SLC, ES-DC-OVA/Lptn, ES-DC-OVA/Mig, and ES-DC-OVA/mock. Therefore, the four double transfectant ES cell clones used in this study originated from the same ES cell clone transfected with the OVA gene.

We acquired DCs from these ES cell transfectant clones and compared their capacity to stimulate the $OVA_{257-264}$-specific and K^b-restricted T cell hybridoma, RF.33.70. As shown in Fig. 3*A*, ES-DC-OVA/SLC, ES-DC-OVA/Lptn, ES-DC-OVA/Mig, ES-DC-OVA, and ES-DC-OVA/mock could stimulate RF33.70 with a comparable efficiency. The amounts of chemokine produced by the

induction of their differentiation to DCs. By sporadic selection with a selection drug, ES cell clones transfected with genes can be propagated while maintaining the capacity to express gene products after their differentiation to DCs. Therefore, one can use ES cell transfectants as an infinite source for genetically modified DCs.

In the present study, using this method, we generated DCs expressing chemokine along with a model Ag, OVA. We determined whether coexpression of T cell-attracting chemokine with antigenic protein by DCs enhanced the capacity to prime Ag-specific CTLs upon in vivo transfer. We also examined the potency of the genetically modified DCs to elicit antitumor immunity against tumor cells expressing OVA. Among T cell-attracting chemokines, we selected SLC, Mig, and Lptn, and comparatively evaluated their effects.

Materials and Methods

Mice

CBA and C57BL/6 mice were obtained from CLEA (Tokyo, Japan) or Charles River Breeding Laboratories (Hamamatsu, Japan) and kept under specific pathogen-free conditions. Male CBA and female C57BL/6 mice were mated to produce (CBA crossed with C57BL/6) F_1 (CBF_1) mice and all in vivo experiments were done with the F_1 mice at 6–8 wk of age.

Cell lines

The ES cell line TT2, derived from (CBA crossed with C57BL/6) F_1 blastocysts (17), were maintained as described (18). The T cell hybridoma RF33.70 (19), recognizing $OVA_{257-264}$ in the context of K^b, and the M-CSF-defective bone marrow-derived stromal cell line, OP9 (20), have been reported. MO4 (21) was generated by transfection of C57BL/6-derived melanoma B16 with the pAc-neo-OVA plasmid, as described (22). The procedure for induction of differentiation of ES cells into DCs has been reported (16), and ES-DCs recovered after a 14-day culture in bacteriological petri dishes were used for in vivo and in vitro assays.

Peptide, cytokines/chemokines, and anti-chemokine Ab

The K^b-binding peptide $OVA_{257-264}$, SIINFEKL, were synthesized using the F-MOC method on an automatic peptide synthesizer (PSSM8; Shimadzu, Kyoto, Japan) then purified by HPLC. Recombinant mouse GM-CSF was provided by Kirin Brewery (Tokyo, Japan). Recombinant mouse SLC, Mig, and Lptn, were purchased from DACO JAPAN (Kyoto, Japan). Goat anti-mouse SLC and Mig Abs and biotinylated goat anti-mouse SLC and Mig Abs were also purchased from DACO JAPAN. Rabbit anti-mouse Lptn Ab was purchased from eBioscience (San Diego, CA), and was biotinylated using a MiniBiotin-XX Protein Labeling kit (F-6347; Molecular Probes, Portland, OR).

cDNA array analysis of chemokine gene expression

BM-DCs were generated from bone marrow cells of CBF_1 mice, as described (23, 24). Total RNA was extracted from BM-DCs on day 12 and ES-DCs on day 14 of culture in bacteriological petri dishes, using RNeasy mini kits (Qiagen, Studio City, CA). Total RNA (3 μg) from each sample was reverse transcribed into cDNA with Moloney murine leukemia virus reverse transcriptase (Promega, Madison, WI) in the presence of [α-^{32}P]dCTP (Amersham Pharmacia Biotech, Piscataway, NJ). The resulting cDNA probes were hybridized to cDNA fragments spotted on GEArray membranes (SuperArray, Bethesda, MD). Hybridization and wash of the membranes were done following the manufacturer's instructions. The intensity of radioactive signaling from the hybridized probes was analyzed on a BAS-2000 (Fujifilm, Tokyo, Japan). The signal from expression of each chemokine gene was normalized to the signal derived from β-actin on the same membrane and expressed as arbitrary units calculated using the formula: Chemokine mRNA arbitrary units = (chemokine signal − background signal)/(β-actin signal − background signal) (25).

Plasmid construction

A cDNA fragment encoding for OVA protein was transferred to pCAG-IP (26), a mammalian expression vector containing the chicken β-actin promoter and an internal ribosomal entry site (IRES)-puromycin *N*-acetyltransferase gene cassette, to generate pCAG-OVA-IP. To obtain pCAGGS-IRES-neo-R, a DNA fragment containing IRES-neomycin-resistant (neo-R) was inserted into a mammalian expression vector pCAGGS (27). A cDNA fragment coding for chemokine protein was inserted into pCAGGS-IRES-neo-R. SLC cDNA was obtained by RT-PCR using murine spleen cells as the RNA source and PCR primers, AACCCTCTAGCCCGCCGCCAC-CATGGCTCAGAGATG ACTCT (forward) and AACCCGGATCCAGGCGGGCTACTACTGGCT ATCC (reverse). Mig cDNA was obtained by RT-PCR using murine spleen cells stimulated for 24 h with IFN-γ as the RNA source and the PCR primers, AACCCTCTAGACCCGCCGCCACCATGAAGTCCGCTGTTCTTTTCC (forward) and AACCCGGATCCAGGGTGCTTGTTGGTAAAG (reverse). Lptn cDNA was obtained by RT-PCR, using murine spleen cells as the RNA source stimulated for 24 h with PMA and A23187 and the PCR primers AAC CCTCTAGACCCGCCGCCACCATGAGACTTCTCCTCCTGAC (forward) and AACCCGGATCCCTGGAGGCTGTTACCCAGTC (reverse). The design of these primers results in cloning of chemokine cDNA downstream of the Kozak sequence (28). The PCR products were cloned into a plasmid vector (pGEM-T easy; Promega), confirmed by sequencing analysis, and then transferred to the expression vector.

Transfection of ES cells and generation of ES-DCs expressing chemokine along with OVA

To generate OVA-transfected ES cell clones, TT2 ES cells were introduced with pCAG-OVA-IP by electroporation and selected with puromycin using the reported procedure (16). OVA-transfected ES cell clones were differentiated to ES-DCs, and an ES cell transfectant clone highly expressing OVA after differentiation to DCs (ES-OVA) was selected, based on the capacity to stimulate RF33.70, the OVA-reacting T cell hybridoma. The selected ES cell clone was transfected with one of three kinds of chemokine expression vectors or pCAGGS-IRES-neo-R (mock). Transfected ES cells were cultured on neo-R primary embryonic fibroblasts feeder layers and selected with G418 (500 μg/ml), and drug-resistant colonies were picked up. Double-transfectant ES cell clones producing high amounts of chemokine after differentiation to DCs were selected. To determine chemokine levels in culture supernatants, ELISAs were done as we reported (29).

T cell hybridoma assay for detection of OVA peptide-K^b complexes

Graded numbers of ES-DCs as stimulators were seeded into 96-well flat-bottom culture plates together with RF33.70 as responders (5×10^4 cells/well in final volume of 200 μl). After 24 h of culture, the supernatant (50 μl/well) was collected and added to culture of the IL-2-dependent cell line, CTLL-20 (5×10^3/100 μl/well), in 96-well flat-bottom culture plates. After 16 h, [^{3}H]thymidine (248 MBq/mmol) was added (37.5 KBq/well) and cells were incubated for a further 8 h. The incorporation of [^{3}H]thymidine by CTLL-20 was measured by scintillation counting.

In vitro survival assay of ES-DCs

ES-DCs recovered from 14-day culture in petri dishes were cultured again in petri dishes (1.2×10^5/90 mm dish) under several conditions. After 7 days, cells were recovered by pipetting, stained with trypan blue and microscopically counted. Some recovered cells were also stained with propidium iodide (10 μg/ml) and analyzed on a flow cytometer (FACScan, BD Biosciences, San Jose CA) to detect dead cells.

Assay of the migration of DCs in vivo

DCs (2×10^6) labeled with 1 μM CFSE (Molecular Probes, Oss, The Netherlands) in serum-free medium for 10 min at 37°C, were i.p. transferred into the CBF_1 mouse. After 40 h, 5-μm frozen sections of the spleen were made and examined under a fluorescence microscope (Olympus, Melville, NY) or stained with H&E. ^{111}In-labeled DCs (1×10^6) were i.p. transferred into mice. After 40 h, several organs were isolated and the radioactivity in each organ was measured on a gamma counter as described by Eggert et al. (6) and Morse et al. (9). The radioactivity was expressed as the percentage of injection dose per 0.1 gram of tissue, so that the values were adjusted to 0.1 g of tissue to correct for weight differences of each organ.

Induction of OVA-specific CTLs in vitro and cytotoxicity assay

ES-DCs (4×10^5/well) or BM-DCs (4×10^5/well) were cocultured with T cells (2.5×10^6/well) purified with a nylon wool column from spleen cells of unprimed CBF_1 mice in 24-well culture plates in RPMI 1640 supplemented with 10% FCS. In some experiments, ES-DCs were killed before use by treatment at 70°C for 20 min. BM-DCs were prepared as described (23) then pulsed with OVA peptide (10 μM) for 4 h, washed twice, and used as stimulators. After 5 days of culture, cells were recovered

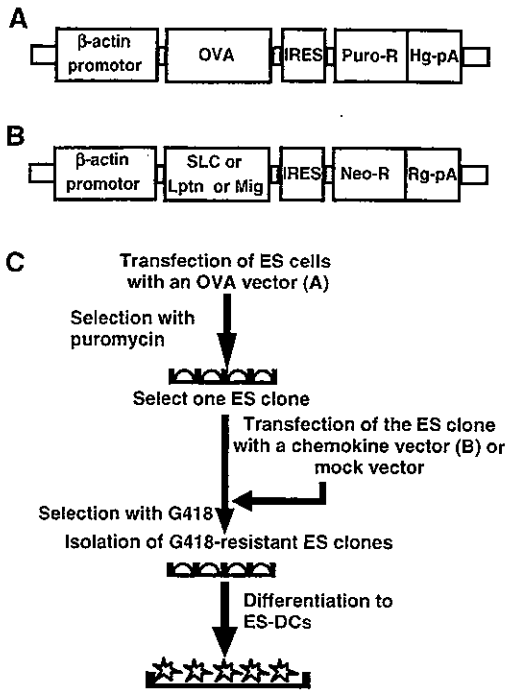

FIGURE 2. Generation of ES-DCs expressing chemokine simultaneously with OVA. *A*, Structure of OVA protein expression vector, pCAG-OVA-PI. The expression of this gene is driven by the chicken β-actin promoter. The OVA protein coding sequence is followed by the IRES-puromycin *N*-acetyltransferase gene (Puro-R) and the polyadenylation signal sequence of human growth hormone (Hg-pA). *B*, Structure of chemokine expression vector, pCAGGS-chemokine-IRES-neo-R. Expression of this gene is driven by the chicken β-actin promoter. The chemokine coding sequence is followed by the IRES-neo-R gene (Neo-R) and a polyadenylation signal sequence of rabbit β-globin poly(A) (Rg-pA). *C*, TT2 ES cells were transfected with pCAG-OVA-PI. Puromycin-resistant colonies were picked up and expanded. An ES cell clone highly expressing OVA was selected and transfected with one of three kinds of pCAGGS-chemokine-IRES-neo-R or with a mock vector. G418-resistant colonies were picked up and expanded. One ES clone expressing large amounts of chemokine after DC differentiation was selected for each chemokine and used in the described experiments.

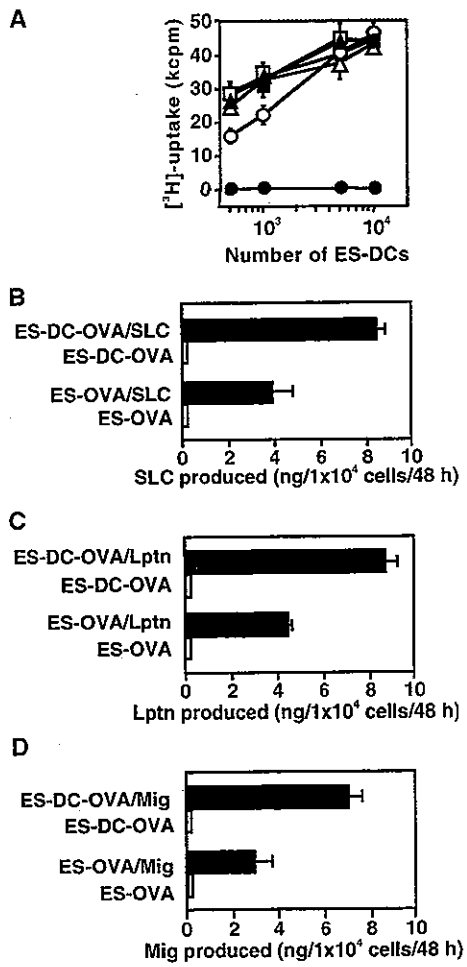

FIGURE 3. Stimulation of OVA-specific T cell hybridoma and chemokine production by genetically modified ES-DCs. *A*, Stimulation of K^b-restricted OVA-specific T cell hybridoma, RF33.70, with ES-DC-OVA (■), ES-DC-OVA/mock (□), ES-DC-OVA/SLC (▲), ES-DC-OVA/Lptn (△), ES-DC-OVA/Mig (○), or negative control, ES-DC-TT2 (●) without OVA-expression, was analyzed. Stimulators and RF33.70 were cocultured for 24 h, and IL-2 produced by RF33.70 was quantified by measuring proliferation of CTLL-20 cells. Results were expressed as mean cpm of triplicate cultures ± SD. Data are representative of three independent and reproducible experiments. *B–D*, The 48-h culture supernatants of the 1×10^6 ES-DC-OVA expressing chemokine or ES-DC-OVA in petri dishes and that of 1×10^6 ES-OVA expressing chemokine or ES-OVA on layers of primary embryonic fibroblasts were harvested. The concentrations of chemokine in the supernatants were measured using ELISA. Production of chemokine SLC (*B*), Lptn (*C*), and Mig (*D*) by respective transfectants was quantified. Results are expressed as mean amounts of chemokine per 1×10^4 cells of triplicate cultures ± SD. Data are representative of two independent and reproducible experiments.

three kinds of chemokine gene-transfected cells used in this study are shown in Fig. 3, *B–D*. Both ES cells and differentiated ES-DCs produced transgene-derived chemokines, and comparable protein amounts of chemokines were produced by the three chemokine gene-transfected ES-DCs. Morphology and surface phenotypes of chemokine gene-transfected ES-DCs were not significantly different from ES-DC-TT2 (DCs derived from parental TT2 ES cells) (data not shown). These results suggest that the forced expression of OVA protein and the chemokines by gene transfer to ES cells do not affect their differentiation to DCs.

The migration capacity of ES-DCs in vivo

To test the migration capacity of ES-DCs in vivo, we histologically examined the migration of transferred ES-DCs to the spleen. In addition, we tested whether or not the expression of SLC, the chemokine with DC-attracting property, by ES-DCs would affect their in vivo migration. As shown in Fig. 4, *A–F*, CFSE-labeled ES-DC-OVA, ES-DC-OVA/SLC, and BM-DCs migrated to the spleen to the same extent, mostly localizing in the white pulp and the marginal zone (Fig. 4, *B*, *D*, and *F*).

We also investigated the distribution of ^{111}In-labeled DCs in lymphoid organs after i.p. transfer. The distribution of ES-DCs shown in Fig. 4*G* indicated that ES-DCs and BM-DCs similarly accumulated in the spleen and mesenteric LN 40 h after the transfer, and that expression of SLC by ES-DCs made no significant difference in the migration pattern.

Collectively, the migratory capacity toward lymphoid tissues of ES-DCs is almost comparable to that of BM-DCs, and the SLC produced by ES-DC-OVA/SLC did not prevent them from migrating toward lymphoid tissues.

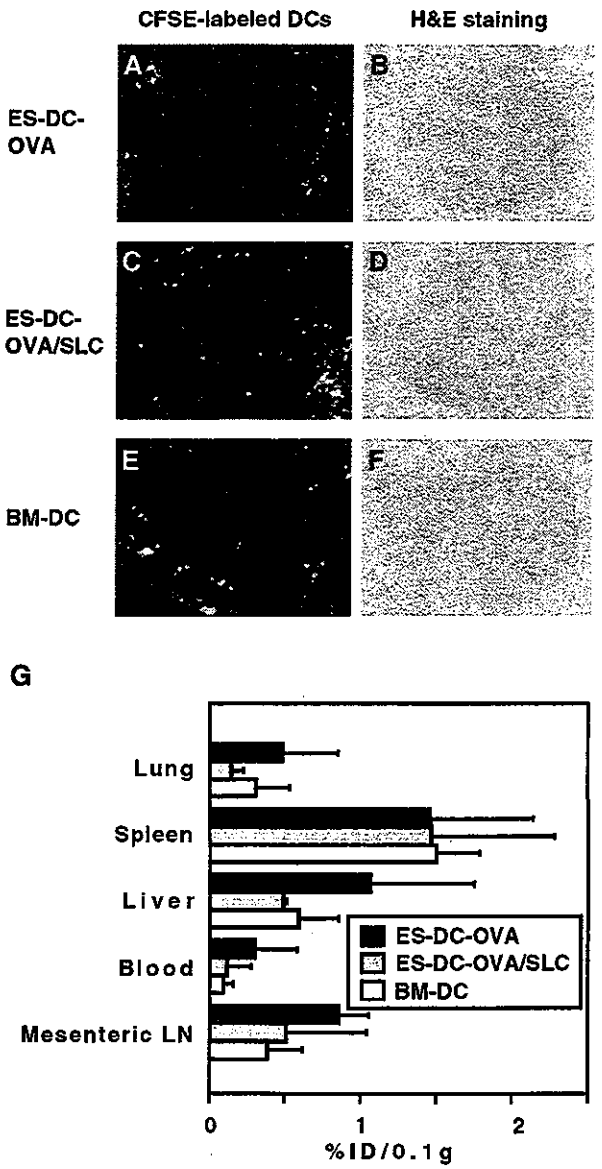

FIGURE 4. The migration capacity of ES-DCs in vivo. *A–F*, DCs (2×10^6) were labeled with CFSE and injected i.p. into mice. At 40 h later, frozen sections of spleens were prepared. Injected DCs were ES-DC-OVA (*A* and *B*), ES-DC-OVA/SLC (*C* and *D*), and BM-DCs (*E* and *F*). *A*, *C*, and *E* are fluorescense images of the sections serial to H&E-stained sections shown in *B*, *D*, and *F*, respectively. *G*, ^{111}In-labeled DCs (1×10^6) were injected i.p. into mice, and radioactivity of indicated organs was measured 40 h later. The measured radioactivity in tissues was expressed as percentage of injection dose per 0.1 g tissue (%ID/0.1 g) as described in *Materials and Methods*. Results were expressed as mean %ID/0.1 g + SD ($n = 3$ per group).

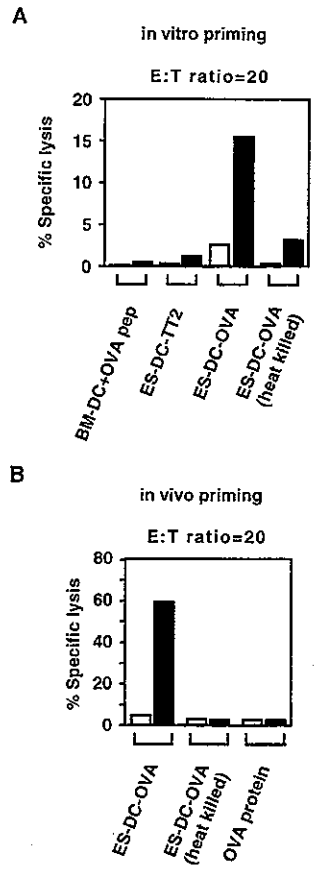

FIGURE 5. Priming of OVA-specific CTLs with genetically modified ES-DCs. *A*, BM-DCs prepulsed with OVA peptide (10 μM), ES-DC-TT2, ES-DC-OVA, or heat-killed ES-DC-OVA were cocultured with splenic T cells of unprimed CBF_1 mice. After 5 days, the resultant cells were assayed for the capacity to kill EL-4 tumor cells either pulsed with 10 μM OVA peptide (■) or left unpulsed (□) at an E:T ratio of 20. *B*, Mice were transferred i.p. twice with ES-DC-OVA (2×10^4), alive or heat killed, or OVA protein (50 μg) on days −14 and −7. Spleen cells were harvested from the mice on day 0, pooled for each group (four mice per group), and cultured in the presence of $OVA_{257-264}$ (0.1 μM) for 5 days. The resultant cells were assayed for the capacity to kill EL-4 tumor cells either pulsed with 10 μM OVA peptide (■) or left unpulsed (□) at an E:T ratio of 20. Results are expressed as mean specific lysis of triplicate assays, and SDs of triplicates were <2%. Data are representative of two independent and reproducible experiments.

Priming of Ag-specific CTLs with genetically modified ES-DCs in vitro and in vivo

We analyzed the capacity of ES-DC-OVA to prime OVA-specific T cells in vitro. ES-DC-TT2, ES-DC-OVA, heat-killed ES-DC-OVA, or BM-DCs prepulsed with OVA peptide were cocultured with splenic T cells derived from unprimed CBF_1 mice. After 5 days, cells were recovered and OVA-specific CTL activity was analyzed. The results shown in Fig. 5*A* indicate that OVA-specific CTLs were primed in vitro by intact ES-DC-OVA but not by ES-DC-TT2, BM-DCs prepulsed with $OVA_{257-264}$ peptide, or heat-killed ES-DC-OVA. BM-DCs prepulsed with OVA peptide could prime OVA-specific CTLs in vitro only in the presence of exogenous IL-2, whereas ES-DC-OVA could prime OVA-specific CTLs, regardless of whether or not IL-2 had been added (our unpublished observations).

Furthermore, the capacity of ES-DC-OVA to prime OVA-specific T cells in vivo was analyzed. ES-DC-OVA (2×10^4), heat-killed ES-DC-OVA (2×10^4), or OVA protein (50 μg) were injected i.p. into CBF_1 mice twice within a 7-day interval. Spleen cells were isolated 7 days after the second injection and then cultured in vitro in the presence of $OVA_{257-264}$ peptide. After 5 days, cells were recovered and assayed for their capacity to kill EL-4 thymoma cells ($H\text{-}2^b$) prepulsed with the OVA peptide. The results shown in Fig. 5*B* indicate that CTLs specific to the OVA epitope were primed in vivo with ES-DC-OVA but not with heat-killed ES-DC-OVA or soluble OVA protein.

These results demonstrated that live ES-DCs genetically modified to express an antigenic protein have the capacity to prime

Ag-specific CTLs both in vitro and in vivo. There is little possibility that endogenous host DCs, which phagocytosed ES-DCs expressing OVA or OVA protein, played a major role in priming CTLs, based on the result that CTLs were not primed either by injection with heat-killed ES-DC-OVA or by OVA protein.

Efficient priming of OVA-specific CTLs by DCs producing chemokine along with OVA

We analyzed the capacity of genetically modified ES-DCs expressing Mig along with OVA to prime OVA-specific T cells in vivo. Graded numbers of ES-DC-OVA or ES-DC-OVA/Mig were transferred i.p. to mice twice at a 7-day interval. Spleen cells were isolated 7 days after the second transfer then cultured in vitro in the presence of $OVA_{257-264}$ peptide. After 5 days, cells were recovered and assayed for their capacity to kill EL-4 thymoma cells ($H\text{-}2^b$) prepulsed with the OVA peptide (Fig. 6). When 5×10^4 or 3×10^4 DCs were transferred twice, a comparable level of OVA-specific CTL activity was primed by ES-DC-OVA and ES-DC-OVA/Mig. In contrast, when 1×10^4 DCs were transferred twice, ES-DC-OVA/Mig primed CTL activity to a greater extent than seen with ES-DC-OVA. As we reported, OVA-specific CTLs were not primed by transfer of ES-DC-TT2, even when 5×10^5 DCs were transferred twice (16).

We next analyzed effects of expression of the three chemokines on in vivo CTL-priming using the same experimental procedure as previously described except that smaller numbers of DCs were transferred into the mice (Fig. 7). When mice were given 5×10^3 ES-DCs twice, all OVA-expressing DCs stimulated OVA-specific CTLs, and the T cell-priming capacity of DCs coexpressing either of the three chemokines was significantly stronger than those expressing OVA alone. Even when only 3×10^3 DCs were transferred twice, OVA-specific CTLs were primed by the three kinds of ES-DC-OVA chemokine. Conversely, priming of CTLs by ES-DCs expressing OVA alone was not detected under this condition.

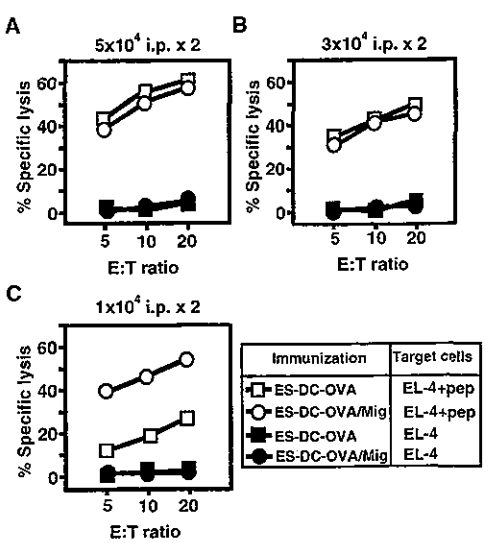

FIGURE 6. Priming of OVA-specific CTLs in vivo by immunization with ES-DC-OVA/Mig. Mice were transferred i.p. twice with ES-DC-OVA or ES-DC-OVA/Mig on days −14 and −7 with 5×10^4 (*A*), 3×10^4 (*B*), or 1×10^4 (*C*) ES-DCs. Spleen cells from transferred mice were harvested on day 0, pooled for each group (three mice per group), and cultured in the presence of $OVA_{257-264}$ (0.1 μM) for 5 days. The resultant cells were assayed for the capacity to kill EL-4 tumor cells either pulsed with 10 μM OVA peptide or left unpulsed. Results are expressed as mean specific lysis of triplicate assays, and SDs of triplicates were <2%. Data are representative of three independent and reproducible experiments.

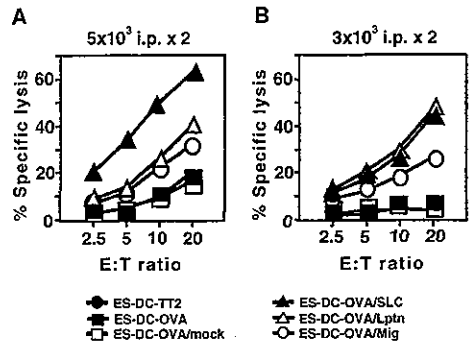

FIGURE 7. Enhanced priming of OVA-specific CTLs in vivo by immunization with ES-DCs expressing chemokine along with OVA. Mice were transferred i.p. twice on days −14 and −7 with 5×10^3 ES-DCs (*A*) or 3×10^3 ES-DCs (*B*). ES-DCs expressing chemokine along with OVA were ES-DC-OVA/SLC (▲), ES-DC-OVA/Lptn (△), ES-DC-OVA/Mig (○). ES-DCs expressing OVA alone as controls were ES-DC-OVA/mock (□) and ES-DC-OVA (■). DCs differentiated from the parental OVA gene single-transfectant ES cell clone. Spleen cells of the mice were isolated on day 0, pooled for each group (three to seven mice per group), and assayed for the CTL activity using the same procedure as in Fig. 5. For all effectors, specific lysis was <2% when target EL-4 cells were not prepulsed with OVA peptide. Results were expressed as mean specific lysis of triplicate assays, and SDs of triplicates were <2%. Data are representative of three independent and reproducible experiments.

These results clearly demonstrate that coexpression of the chemokines along with Ag in DCs enhances their capacity to prime the Ag-specific CTLs in vivo. The results shown in Fig. 7 also indicate that coexpression of SLC or Lptn in DCs is more effective than that of Mig in the priming of CTLs in vivo.

Protective effects of immunization with chemokine gene-modified DCs against tumor cell challenge

We next asked whether coexpression of chemokine with OVA in DCs would enhance their capacity to induce protective immunity against tumor cells expressing OVA. We immunized mice by twice i.p. transfers of DCs at 7-day intervals, and 7 days after the second transfer, the mice were challenged s.c. with 3×10^5 MO4 cells, OVA-expressing melanoma cells derived from B16. In case of two transfers of 3×10^3 ES-DCs, as shown in Fig. 8*A*, immunization with ES-DCs expressing OVA alone (ES-DC-OVA/mock) provided significant protection against the MO4 challenge, in comparison with ES-DC-TT2 ($p < 0.01$). Conversely, transfer of ES-DC-TT2 gave no significant protection, compared with no DC transfer (data not shown). Immunization with ES-DC-OVA/SLC provided greater protection than did immunization with ES-DC-OVA/mock ($p < 0.05$). In contrast, protection given by immunization with ES-DC-OVA/Mig or ES-DC-OVA/Lptn was at a comparable level to that provided by ES-DC-OVA/mock. As shown in Fig. 8*B*, immunization with ES-DC-OVA/mock showed a significant prolongation of survival, compared with immunization with ES-DC-TT2 ($p < 0.05$). Immunization with ES-DC-OVA/SLC resulted in a further prolongation of survival. However, coexpression of Lptn or Mig had no significant additive effect on survival.

In case of twice transfers of 2×10^4 ES-DCs, as shown in Fig. 8*C*, immunization with ES-DC-OVA/mock provided significant protection against MO4 challenge, compared with ES-DC-TT2 ($p < 0.01$). Under this condition, immunization with ES-DC-OVA/SLC and ES-DC-OVA/Mig provided greater protection than that seen with ES-DC-OVA/mock ($p < 0.05$). In contrast, effect of immunization with ES-DC-OVA/Lptn was comparable to that of

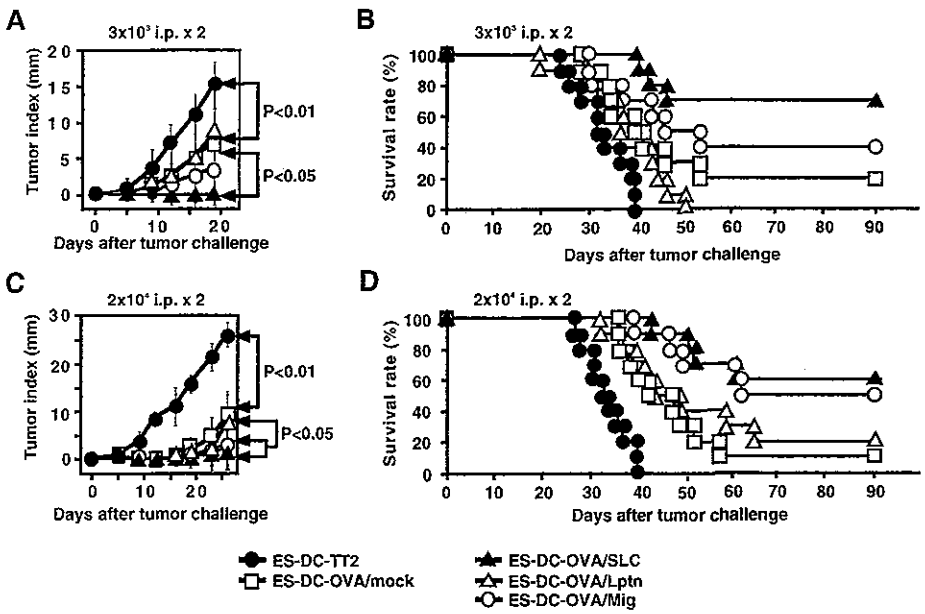

FIGURE 8. Suppression of tumor growth and prolongation of survival by immunization with ES-DCs expressing chemokine along with OVA. Mice were transferred i.p. twice on day −14 and −7 with 3×10^3 (*A* and *B*) or 2×10^4 ES-DCs (*C* and *D*). The mice were challenged s.c. with 3×10^5 MO4 tumor cells expressing OVA on day 0. Tumor index (*A* and *C*) and survival rate (*B* and *D*) were monitored. The differences in tumor index between ES-DC-TT2 and ES-DC-OVA/mock as well as between ES-DC-OVA/mock and ES-DC-OVA/SLC are statistically significant ($p < 0.01$ and $p < 0.05$, respectively) (*A*). The differences in survival rates between ES-DC-TT2 and ES-DC-OVA/mock as well as between ES-DC-OVA/mock and ES-DC-OVA/SLC are statistically significant ($p < 0.05$) (*B*). The difference in tumor index between ES-DC-TT2 and ES-DC-OVA/mock is statistically significant ($p < 0.01$) (*C*). The differences in tumor index between ES-DC-OVA/mock and ES-DC-OVA/Mig as well as between ES-DC-OVA/mock and ES-DC-OVA/SLC are also statistically significant ($p < 0.05$) (*C*). The differences in survival rate between ES-DC-TT2 and ES-DC-OVA/mock as well as between ES-DC-OVA/mock and ES-DC-OVA/SLC are statistically significant ($p < 0.01$) (*D*). The difference in survival rate between ES-DC-OVA/mock and ES-DC-OVA/Mig is also statistically significant ($p < 0.05$) (*D*). *A* and *C*, Results are expressed as mean tumor index ± SD ($n = 10$ per group). *B* and *D*, Kaplan-Meier plot depicts the survival rate ($n = 10$ per group).

ES-DC-OVA/mock. As shown in Fig. 8*D*, immunization with ES-DC-OVA/SLC resulted in a longer survival time than that seen with ES-DC-OVA/mock ($p < 0.01$). In addition, ES-DC-OVA/Mig was more effective than ES-DC-OVA/mock ($p < 0.05$), but less effective than ES-DC-OVA/SLC. Immunization with ES-DC-OVA/Lptn again resulted in survival at the same level as seen with ES-DC-OVA/mock. When mice were twice transferred with 2×10^4 ES-DCs and challenged with 3×10^6 MO4 tumor cells, among the three chemokine-expressing ES-DCs, only immunization with ES-DC-OVA/SLC was more effective than ES-DC-OVA/mock (data not shown).

Collectively, ES-DC-OVA/SLC was always more effective than ES-DC-OVA/mock. Expression of Mig in ES-DC increased survival time under some experimental conditions. In contrast, ES-DC-OVA/Lptn did not elicit more protection than did ES-DC-OVA/mock under the conditions we tested. These results suggest that expression of SLC along with antigenic protein is the most effective among the three chemokines for induction of protective immunity against tumor cells expressing the Ag.

No effect of SLC simultaneously injected with ES-DCs

As described, coexpression of SLC along with OVA in ES-DCs enhanced their capacity to induce protective immunity against tumor cells expressing OVA (Fig. 8). To examine the effect of SLC upon simultaneous injection with ES-DCs expressing OVA, we compared immunization with 2×10^4 ES-DC-OVA/SLC to immunization with 2×10^4 ES-DC-OVA/mock accompanying i.p. or systemic (i.v.) injection of recombinant mouse SLC (3 μg). The amount of injected recombinant mouse SLC was much higher than that expected to be produced by injected ES-DC-OVA/SLC after the transfer (Fig. 3*B*). Transfer of ES-DCs and tumor cell challenge with 3×10^5 MO4 cells were done using the same schedule as previously described. The tumor index in millimeters 30 days after MO4 challenge is shown in Fig. 9. In case of cotransfer of recombinant mouse SLC i.p. or i.v. with ES-DC-OVA/mock, tumor indexes were similar

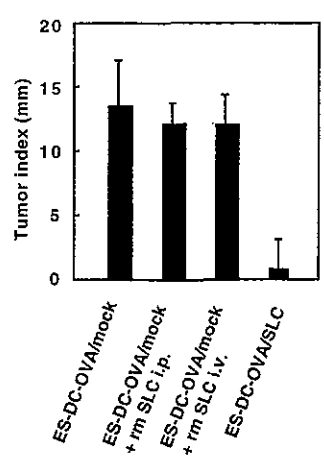

FIGURE 9. No effect of simultaneous injection of recombinant mouse SLC together with ES-DC-OVA. Mice were immunized with ES-DC-OVA/mock (2×10^4/mouse) with or without simultaneous injection of recombinant mouse SLC (3 μg, i.v. or i.p.). Other mice were immunized with ES-DC-OVA/SLC (2×10^4/mouse). Transfers of ES-DCs plus SLC were done twice at a 7-day interval, and 7 days after the second transfer, mice were challenged with 3×10^5 MO4 cells. The tumor index (in millimeters) 30 days after the MO4 challenge was shown. In mice immunized with ES-DC-OVA/SLC, the tumor index was significantly smaller than the others ($p < 0.05$). Results are expressed as mean tumor index + SD ($n = 4$–6 per group).

to those in case of immunization with 2×10^4 ES-DC-OVA/mock, indicating that coinjection of recombinant mouse SLC was without effect. In contrast, in case of immunization with ES-DC-OVA/SLC, the tumor index was significantly smaller than those in other conditions ($p < 0.05$), such being consistent with the data shown in Fig. 8.

No effect of SLC on survival of ES-DCs and on CTL priming activity of ES-DC in vitro

We tested to see whether the SLC would have any effect on the survival of DCs in vitro. ES-DC-OVA/mock and ES-DC-OVA/SLC were cultured for 7 days. Other ES-DC-OVA/mock were cultured in the presence of recombinant mouse SLC (300 ng/ml). Numbers of recovered ES-DCs after the culture were 77.8%, 88.3%, and 77.7% of the starting cells in case of ES-DC-OVA/mock, ES-DC-OVA/SLC, and ES-DC-OVA/mock plus recombinant mouse SLC, respectively. Dead cells were fewer than 1% of the recovered cells under any conditions. These results indicate that the SLC have no significant effect on the survival of DCs in vitro. In addition, there was no difference in the in vitro CTL-priming capacity between ES-DC-OVA and ES-DC-OVA/SLC (Fig. 10). These results suggest that the enhanced CTL-priming by ES-DC-OVA/SLC observed in case of in vivo injection is not due to the direct effect of SLC on ES-DCs.

Involvement of both $CD4^+$ and $CD8^+$ T cells in protection against MO4 induced by ES-DCs expressing OVA

To determine the role of $CD4^+$ and $CD8^+$ T cells in protection against tumor cells induced by genetically modified ES-DCs, we depleted mice of $CD4^+$ or $CD8^+$ T lymphocytes by treatment with anti-CD4 or anti-CD8 mAb in vivo, respectively. By this treatment, >90% of $CD4^+$ and $CD8^+$ T cells were depleted (data not shown). During this procedure, mice were immunized with ES-DC-OVA/SLC or ES-DC-OVA/mock and challenged with MO4 cells. As shown in Fig. 11, depletion of either $CD4^+$ or $CD8^+$ T cells totally abrogated the protective immunity induced by ES-DC-OVA/SLC or ES-DC-OVA/mock. Although some populations of physiological DCs have been reported to express CD4 or CD8 molecules, the number of $CD11c^+$ splenic DCs did not change with this treatment (data not shown), indicating that the abrogation

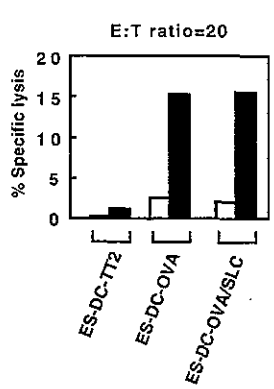

FIGURE 10. Similar capacity of ES-DC-OVA and ES-DC-OVA/SLC to prime OVA-specific CTLs in vitro. ES-DC-TT2, ES-DC-OVA, and ES-DC-OVA/SLC (4×10^5/well) were cocultured with nylon wool-purified splenic T cells (2.5×10^6/well) of unprimed CBF_1 mice in 24-well culture plates. After 5 days, the cells were harvested and assayed for the capacity to kill EL-4 tumor cells either pulsed with 10 μM OVA peptide (■) or left unpulsed (□). Results are expressed as mean specific lysis of triplicate assays, and SDs of triplicates were <2%. Data are representative of two independent and reproducible experiments.

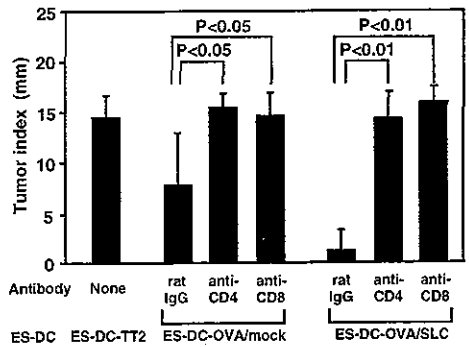

FIGURE 11. Involvement of both $CD4^+$ and $CD8^+$ T cells in antitumor immunity induced by ES-DCs. $CD4^+$ or $CD8^+$ T cells were depleted in vivo by inoculation of anti-$CD4^+$ or anti-$CD8^+$ mAbs during immunization with ES-DC-OVA/mock or ES-DC-OVA/SLC. As control, other mice were given i.p. by transfer of ES-DC-TT2. The mice were challenged s.c. with 3×10^6 MO4 tumor cells, and tumor measurements were made 15 days after the tumor cell challenge. In case of immunization with ES-DC-OVA/mock, the differences in tumor index between mice inoculated with rat IgG and those with anti-CD4 mAb as well as between mice inoculated with rat IgG and those with anti-CD8 mAb are statistically significant ($p < 0.05$). In case of immunization with ES-DC-OVA/SLC, the differences in tumor index between mice inoculated with rat IgG and those with anti-CD4 mAb as well as between mice inoculated with rat IgG and those with anti-CD8 mAb are statistically significant ($p < 0.01$). Results were expressed as mean tumor index + SD ($n = 8$ per group).

of protective immunity by Ab treatment is due to the depletion of T cells and not due to the effect on endogenous host DCs. These results suggest that both $CD4^+$ and $CD8^+$ T cells play critical roles in antitumor immunity induced by OVA-expressing DCs, regardless of whether or not they coexpress SLC.

We histologically investigated the tumor tissues to search for infiltration of lymphocytes. As shown in Fig. 12, *A–F*, the size of the tumor in mice immunized with ES-DC-OVA/SLC was much smaller than that of mice immunized with ES-DC-OVA/mock or ES-DC without OVA (ES-DC-TT2). There was a large number of inflammatory cells infiltrating into tumor tissues of mice immunized with ES-DCs expressing OVA, particularly in mice immunized with ES-DC-OVA/SLC. The infiltrating cells consisted of both $CD4^+$ and $CD8^+$ T cells (Fig. 12, *G* and *H*). These results also suggest that the antitumor effect induced by ES-DC expressing SLC along with OVA is mediated by both $CD4^+$ and $CD8^+$ T cells.

Discussion

In the present study, we attempted to improve the capacity of in vivo transferred DCs to prime T cells by genetic modification to express a chemokine with a T cell-attracting property. Among the chemokines, we comparatively evaluated the effects of three chemokines, SLC, Mig, and Lptn, not produced by DCs under physiological conditions. For the genetic modification of DCs, we used a method to generate DCs from mouse ES cells. By sequential transfection of ES cells with expression vectors for OVA Ag and for chemokines and by subsequent induction of differentiation to DCs, we generated DCs expressing a chemokine along with OVA.

ES-DCs have a migratory capacity toward lymphoid tissues (Fig. 4) and the capacity is almost comparable to that of BM-DCs. ES-DCs expressing OVA could induce the Ag-specific priming of CTLs both in vivo and in vitro (Fig. 5). ES-DCs expressing OVA could prime OVA-specific CTLs in the absence of IL-2 in vitro, whereas stimulation with CD40 ligand (30) or presence of exogenous IL-2 (our unpublished observations) is essential for BM-DCs to prime Ag-specific CTLs in vitro. Therefore, the capacity of

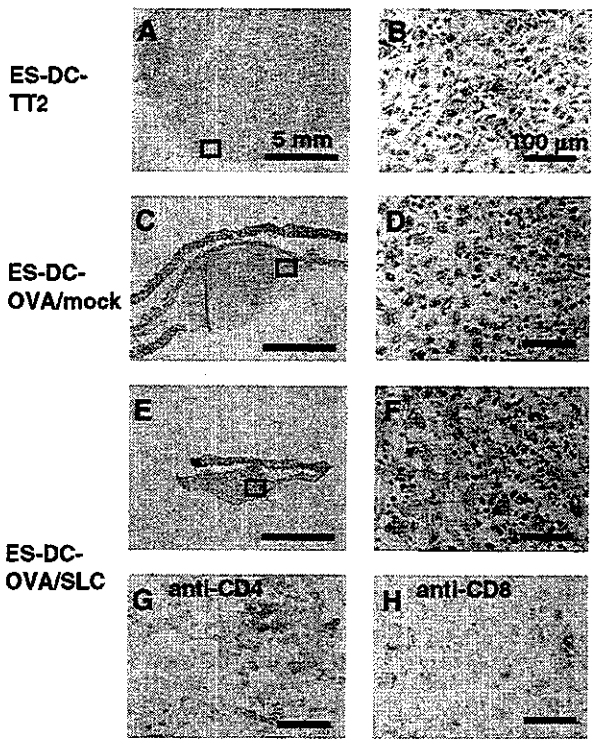

FIGURE 12. Infiltration of both $CD4^+$ and $CD8^+$ T cells into tumor tissues. Mice were transferred twice with ES-DC-TT2 (*A* and *B*), ES-DC-OVA/mock (*C* and *D*), or ES-DC-OVA/SLC (*E–H*). Seven days after the second transfer, mice were challenged with 3×10^6 MO4 tumor cells. Twelve days after the tumor cell challenge, frozen sections of tumor tissues were made and stained with H&E (*A–F*) or immunostained with anti-CD4 (*G*) or anti-CD8 (*H*) mAb. *F–H*, Serial sections are shown. *B*, *D*, and *F*, Enlarged views of the portion indicated in the square of *A*, *C*, and *E*, respectively. Note that size of the tumor in mice immunized with ES-DC-OVA/SLC (*E*) was much smaller than that of mice immunized with ES-DC-TT2 (*A*) and ES-DC-OVA/mock (*C*). Scale bars are 5 mm (*A*, *C*, and *E*) and 100 μm (*B*, *D*, *F*, *G*, and *H*).

Ag-expressing ES-DCs to induce CTLs specific to the Ag is no way inferior to BM-DCs. Recently, several reports suggested transfer of Ag or peptide-MHC complexes from adoptively transferred DCs to endogenous host DCs (8, 31). Therefore, it is possible that intrinsic host DCs played some role also in priming of CTLs in our system. However, based on the finding that transfer of heat-killed ES-DC-OVA did not induce priming of CTLs (Fig. 5*B*), we consider that the OVA-specific CTL-priming in our system mainly depends on the direct action of injected ES-DCs expressing OVA.

Among the three chemokines, expression of SLC was the most effective in eliciting protection against OVA-expressing tumor cells (Fig. 8). However, simultaneous injection of recombinant mouse SLC i.p. or i.v. together with an i.p. injection of DCs expressing OVA had no significant additive effect on protection against tumor (Fig. 9). In addition, SLC had no significant effect on the survival of DCs and CTL-priming capacity in vitro (Fig. 10). These results suggest that the enhanced immunizing effect of ES-DC-OVA/SLC observed with in vivo transfer is not due to the effect of SLC on ES-DCs but rather due to attraction of T cells to the site of transferred ES-DCs, and emphasize the significance of the production of the chemokine by DCs.

We consider that antitumor effects induced by transfer of ES-DCs expressing OVA are primarily mediated by $CD4^+$ and $CD8^+$ T cells reacting to OVA. This notion is supported by findings that the antitumor effect was abrogated by depletion of either $CD4^+$ or $CD8^+$ T cells by treatment with specific mAbs in vivo (Fig. 11). In addition, immunohistochemical analyses demonstrated obvious infiltration of both $CD8^+$ and $CD4^+$ T cells into tumor tissues in mice immunized with ES-DC-OVA/SLC (Fig. 12). The total abrogation of antitumor effects upon challenge with B16 tumor cells or derivative cells not only by depletion of $CD8^+$ T cells but also by depletion of $CD4^+$ T cells is consistent with reported data (32–34). In addition to providing aid for activation of $CD8^+$ T cells, $CD4^+$ T cells may directly attack B16 or MO4 cells that express MHC class II molecules upon stimulation with IFN-γ (33).

Expression of Lptn in DCs enhanced CTL priming no less effectively than that of Mig. In contrast, expression of Lptn in DCs did not result in any significant enhancement of protection against tumor challenge. This observation is inconsistent with the report by Cao et al. (35) that showed the effect of expression of Lptn in peptide Ag-pulsed DCs on promoting protective antitumor immunity. The discrepancy between their report and ours may be attributed to retention of OVA-specific activated T cells nearby transferred ES-DC-OVA/Lptn in our experiments. Lptn attracts memory or activated rather than naive T cells (36). We consider that, under our experimental conditions, significant numbers of OVA-specific T cells primed with DCs transferred by the first transfer were particularly attracted toward ES-DCs expressing Lptn transferred by the second transfer, which was given 7 days before the tumor challenge, and the T cells could not efficiently migrate to site of the tumor cell inoculation. Although this speculation has not been experimentally verified, the selective attraction of effector/memory T cells by Lptn could be beneficial when we attempt to down-modulate immune responses by genetically modified ES-DCs, aiming at treatment of autoimmune diseases, and allergy or prevention of transplant rejection.

Although it has been demonstrated that SLC gene-introduced and tumor cell lysate-loaded DCs promoted strong antitumor responses (37), ours is the first study to comparatively evaluate effects of three chemokines. We generated DCs expressing chemokine simultaneously with antigenic protein. For induction of antitumor immunity, gene-based Ag-expression by DC is considered superior to peptide, protein, or cell lysate-loading in DC-based immunization. The expression of genes encoding for entire tumor-specific Ags circumvents the need for identification of specific CTL epitopes within the protein (38). Expression of tumor-specific Ags within DCs provides a continuous and renewable supply of Ags for presentation, as opposed to a single pulse of peptides or tumor cell lysates. In fact, in the current study, transfer of genetically modified ES-DCs (3×10^3 crossed two times) elicited significant CTL responses and protection against tumor challenge. Numerous tumor-associated Ags have been identified by investigators including us (39–41). We are planning to test antitumor effects of the newly identified natural tumor Ags in in vivo experiments using genetically modified ES-DCs expressing the Ags.

As for the methods for gene transfer to DCs, electroporation, lipofection, and virus vector-mediated transfection have been developed. Many clinical trials using DCs transfected with virus-based vectors are now in progress. However, there are several problems related to the presently used strategies, i.e., efficiency of gene transfer, stability of gene expression, potential risk accompanying the use of virus vectors, and immunogenicity of virus vectors. Although improvements have been made in these methods (42, 43), development of more efficient and safer means is needed. For ES cells, efficient methods for gene-transfer and for isolation of appropriate recombinant cell clones have been established. In the present study, we introduced ES cells sequentially with two

expression vectors containing puromycin-resistant and neo-R genes. It should be feasible to generate more than triple-gene transfectant ES-DCs by sequential or simultaneous transfection with multiple expression vectors, or by using an exchangeable gene-trap system (16, 44). Although formation of teratomas accompanying the transfer of ES cell-derived cells may be anticipated (45), we observed no apparent abnormality, including teratoma formation in mice transferred with ES-DCs 300 days before. When we tested our in vitro differentiation protocol with ES cell lines other than TT2 cells, we observed that DCs can be generated from all of these lines, which included ES cell lines of 129 and C57BL/6 mice origin. We are now planning to generate DCs expressing immunoregulatory molecules along with antigenic proteins, attempting Ag-specific immunosuppression as well as immunostimulation.

A method was established to generate mouse ES cell lines of an appropriate genetic background by nuclear transfer from allogeneic somatic cells to already established ES cell lines (46, 47). Recently, differentiation of hematopoietic cells from human and monkey ES cells has been reported (48, 49). Generation of DCs from human ES cells should also be feasible. With advances in the ES cell-related technologies, immunomodulation by genetically engineered ES-DCs may be applied to the treatment of autoimmune diseases and allergy, prevention of rejection of transplanted organs, and antitumor immunotherapy.

Acknowledgments

We thank Dr. H. Nomiyama (Kumamoto University) for valuable suggestions, Dr. S. Aizawa (Riken Center for Developmental Biology, Kobe, Japan) for TT2, Drs. N. Takakura (Kanazawa University, Kanazawa, Japan) and T. Suda (Keio University, Tokyo, Japan) for OP9, Dr. K. Lock (University of Massachusetts Medical Center) for RF33.70 and MO4, Dr. H. Niwa (Riken Center for Developmental Biology, Kobe, Japan) for pCAG-IP, T. Kubo for technical assistance, and Kirin Brewery for recombinant mouse GM-CSF. M. Ohara (Fukuoka, Japan) provided helpful comments on the manuscript.

References

1. Smithers, M., K. O'Connell, S. MacFadyen, M. Chambers, K. Greenwood, A. Boyce, I. Abdul-Jabbar, K. Barker, K. Grimmett, E. Walpole, and R. Thomas. 2003. Clinical response after intradermal immature dendritic cell vaccination in metastatic melanoma is associated with immune response to particulate antigen. *Cancer Immunol. Immunother. 52:41.*
2. Marten, A., D. Flieger, S. Renoth, S. Weineck, P. Albers, M. Compes, B. Schottker, C. Ziske, S. Engelhart, P. Hanfland, et al. 2002. Therapeutic vaccination against metastatic renal cell carcinoma by autologous dendritic cells: preclinical results and outcome of a first clinical phase I/II trial. *Cancer Immunol. Immunother. 51:637.*
3. Butterfield, L. H., A. Ribas, V. B. Dissette, S. N. Amarnani, H. T. Vu, D. Oseguera, H. J. Wang, R. M. Elashoff, W. H. McBride, B. Mukherji, et al. 2003. Determinant spreading associated with clinical response in dendritic cell-based immunotherapy for malignant melanoma. *Clin. Cancer Res. 9:998.*
4. Stift, A., J. Friedl, P. Dubsky, T. Bachleitner-Hofmann, G. Schueller, T. Zontsich, T. Benkoe, K. Radelbauer, C. Brostjan, R. Jakesz, and M. Gnant. 2003. Dendritic cell-based vaccination in solid cancer. *J. Clin. Oncol. 21:135.*
5. Randolph, G. J., K. Inaba, D. F. Robbiani, R. M. Steinman, and W. A. Muller. 1999. Differentiation of phagocytic monocytes into lymph node dendritic cells in vivo. *Immunity 11:753.*
6. Eggert, A. A., M. W. Schreurs, O. C. Boerman, W. J. Oyen, A. J. de Boer, C. J. Punt, C. G. Figdor, and G. J. Adema. 1999. Biodistribution and vaccine efficiency of murine dendritic cells are dependent on the route of administration. *Cancer Res. 59:3340.*
7. Hermans, I. F., D. S. Ritchie, J. Yang, J. M. Roberts, and F. Ronchese. 2000. $CD8^+$ T cell-dependent elimination of dendritic cells in vivo limits the induction of antitumor immunity. *J. Immunol. 164:3095.*
8. Smith, A. L., and B. Fazekas de St Groth. 1999. Antigen-pulsed $CD8\alpha^+$ dendritic cells generate an immune response after subcutaneous injection without homing to the draining lymph node. *J. Exp. Med. 189:593.*
9. Morse, M. A., R. E. Coleman, G. Akabani, N. Niehaus, D. Coleman, and H. K. Lyerly. 1999. Migration of human dendritic cells after injection in patients with metastatic malignancies. *Cancer Res. 59:56.*
10. Nagira, M., T. Imai, R. Yoshida, S. Takagi, M. Iwasaki, M. Baba, Y. Tabira, J. Akagi, H. Nomiyama, and O. Yoshie. 1998. A lymphocyte-specific CC chemokine, secondary lymphoid tissue chemokine (SLC), is a highly efficient chemoattractant for B cells and activated T cells. *Eur. J. Immunol. 28:1516.*
11. Kim, C. H., L. M. Pelus, E. Appelbaum, K. Johanson, N. Anzai, and H. E. Broxmeyer. 1999. CCR7 ligands, SLC/6Ckine/Exodus2/TCA4 and CKβ-11/MIP-3β/ELC, are chemoattractants for $CD56^+CD16^-$ NK cells and late stage lymphoid progenitors. *Cell. Immunol. 193:226.*
12. Kellermann, S. A., S. Hudak, E. R. Oldham, Y. J. Liu, and L. M. McEvoy. 1999. The CC chemokine receptor-7 ligands 6Ckine and macrophage inflammatory protein-3β are potent chemoattractants for in vitro- and in vivo-derived dendritic cells. *J. Immunol. 162:3859.*
13. Farber, J. M. 1997. Mig and IP-10: CXC chemokines that target lymphocytes. *J. Leukocyte Biol. 61:246.*
14. Hedrick, J. A., and A. Zlotnik. 1997. Identification and characterization of a novel beta chemokine containing six conserved cysteines. *J. Immunol. 159:1589.*
15. Kelner, G. S., J. Kennedy, K. B. Bacon, S. Kleyensteuber, D. A. Largaespada, N. A. Jenkins, N. G. Copeland, J. F. Bazan, K. W. Moore, T. J. Schall, et al. 1994. Lymphotactin: a cytokine that represents a new class of chemokine. *Science 266:1395.*
16. Senju, S., S. Hirata, H. Matsuyoshi, M. Masuda, Y. Uemura, K. Araki, K. Yamamura, and Y. Nishimura. 2003. Generation and genetic modification of dendritic cells derived from mouse embryonic stem cells. *Blood 101:3501.*
17. Yagi, T., T. Tokunaga, Y. Furuta, S. Nada, M. Yoshida, T. Tsukada, Y. Saga, N. Takeda, Y. Ikawa, and S. Aizawa. 1993. A novel ES cell line, TT2, with high germline-differentiating potency. *Anal. Biochem. 214:70.*
18. Senju, S., K. Iyama, H. Kudo, S. Aizawa, and Y. Nishimura. 2000. Immunocytochemical analyses and targeted gene disruption of GTPBP1. *Mol. Cell. Biol. 20:6195.*
19. Grant, E. P., and K. L. Rock. 1992. MHC class I-restricted presentation of exogenous antigen by thymic antigen-presenting cells in vitro and in vivo. *J. Immunol. 148:13.*
20. Kodama, H., M. Nose, S. Niida, and S. Nishikawa. 1994. Involvement of the c-kit receptor in the adhesion of hematopoietic stem cells to stromal cells. *Exp. Hematol. 22:979.*
21. Falo, L. D., Jr., M. Kovacsovics-Bankowski, K. Thompson, and K. L. Rock. 1995. Targeting antigen into the phagocytic pathway in vivo induces protective tumour immunity. *Nat. Med. 1:649.*
22. Moore, M. W., F. R. Carbone, and M. J. Bevan. 1988. Introduction of soluble protein into the class I pathway of antigen processing and presentation. *Cell 54:777.*
23. Inaba, K., M. Inaba, N. Romani, H. Aya, M. Deguchi, S. Ikehara, S. Muramatsu, and R. M. Steinman. 1992. Generation of large numbers of dendritic cells from mouse bone marrow cultures supplemented with granulocyte/macrophage colony-stimulating factor. *J. Exp. Med. 176:1693.*
24. Lutz, M. B., N. Kukutsch, A. L. Ogilvie, S. Rossner, F. Koch, N. Romani, and G. Schuler. 1999. An advanced culture method for generating large quantities of highly pure dendritic cells from mouse bone marrow. *J. Immunol. Methods 223:77.*
25. Chapoval, A. I., J. Ni, J. S. Lau, R. A. Wilcox, D. B. Flies, D. Liu, H. Dong, G. L. Sica, G. Zhu, K. Tamada, and L. Chen. 2001. B7-H3: a costimulatory molecule for T cell activation and IFN-γ production. *Nat. Immun. 2:269.*
26. Niwa, H., S. Masui, I. Chambers, A. G. Smith, and J. Miyazaki. 2002. Phenotypic complementation establishes requirements for specific POU domain and generic transactivation function of Oct-3/4 in embryonic stem cells. *Mol. Cell. Biol. 22:1526.*
27. Niwa, H., K. Yamamura, and J. Miyazaki. 1991. Efficient selection for high-expression transfectants with a novel eukaryotic vector. *Gene 108:193.*
28. Kozak, M. 1990. Downstream secondary structure facilitates recognition of initiator codons by eukaryotic ribosomes. *Proc. Natl. Acad. Sci. USA 87:8301.*
29. Uemura, Y., S. Senju, K. Maenaka, L. K. Iwai, S. Fujii, H. Tabata, H. Tsukamoto, S. Hirata, Y. Z. Chen, and Y. Nishimura. 2003. Systematic analysis of the combinatorial nature of epitopes recognized by TCR leads to identification of mimicry epitopes for glutamic acid decarboxylase 65-specific TCRs. *J. Immunol. 170:947.*
30. Kelleher, M., and P. C. Beverley. 2001. Lipopolysaccharide modulation of dendritic cells is insufficient to mature dendritic cells to generate CTLs from naive polyclonal $CD8^+$ T cells in vitro, whereas CD40 ligation is essential. *J. Immunol. 167:6247.*
31. Kleindienst, P., and T. Brocker. 2003. Endogenous dendritic cells are required for amplification of T cell responses induced by dendritic cell vaccines in vivo. *J. Immunol. 170:2817.*
32. Tuting, T., J. Steitz, J. Bruck, A. Gambotto, K. Steinbrink, A. B. DeLeo, P. Robbins, J. Knop, and A. H. Enk. 1999. Dendritic cell-based genetic immunization in mice with a recombinant adenovirus encoding murine TRP2 induces effective anti-melanoma immunity. *J. Gen. Med. 1:400.*
33. Bohm, W., S. Thoma, F. Leithauser, P. Moller, R. Schirmbeck, and J. Reimann. 1998. T cell-mediated, IFN-γ-facilitated rejection of murine B16 melanomas. *J. Immunol. 161:897.*
34. Cao, X., W. Zhang, J. Wang, M. Zhang, X. Huang, H. Hamada, and W. Chen. 1999. Therapy of established tumour with a hybrid cellular vaccine generated by using granulocyte-macrophage colony-stimulating factor genetically modified dendritic cells. *Immunology 97:616.*
35. Cao, X., W. Zhang, L. He, Z. Xie, S. Ma, Q. Tao, Y. Yu, H. Hamada, and J. Wang. 1998. Lymphotactin gene-modified bone marrow dendritic cells act as more potent adjuvants for peptide delivery to induce specific antitumor immunity. *J. Immunol. 161:6238.*
36. Kurt, R. A., M. Bauck, S. Harma, K. McCulloch, A. Baher, and W. J. Urba. 2001. Role of C chemokine lymphotactin in mediating recruitment of antigen-specific $CD62L^{low}$ cells in vitro and in vivo. *Cell. Immunol. 209:83.*

37. Kirk, C. J., D. Hartigan-O'Connor, B. J. Nickoloff, J. S. Chamberlain, M. Giedlin, L. Aukerman, and J. J. Mule. 2001. T cell-dependent antitumor immunity mediated by secondary lymphoid tissue chemokine: augmentation of dendritic cell-based immunotherapy. *Cancer Res. 61:2062.*
38. Kaplan, J. M., Q. Yu, S. T. Piraino, S. E. Pennington, S. Shankara, L. A. Woodworth, and B. L. Roberts. 1999. Induction of antitumor immunity with dendritic cells transduced with adenovirus vector-encoding endogenous tumor-associated antigens. *J. Immunol. 163:699.*
39. Monji, M., S. Senju, T. Nakatsura, K. Yamada, M. Sawatsubashi, A. Inokuchi, and Y. Nishimura. 2002. Head and neck cancer antigens recognized by the humoral immune system. *Biochem. Biophys. Res. Commun. 294:734.*
40. Nakatsura, T., S. Senju, M. Ito, Y. Nishimura, and K. Itoh. 2002. Cellular and humoral immune responses to a human pancreatic cancer antigen, coactosin-like protein, originally defined by the SEREX method. *Eur. J. Immunol. 32:826.*
41. Nakatsura, T., S. Senju, K. Yamada, T. Jotsuka, M. Ogawa, and Y. Nishimura. 2001. Gene cloning of immunogenic antigens overexpressed in pancreatic cancer. *Biochem. Biophys. Res. Commun. 281:936.*
42. Van Tendeloo, V. F., P. Ponsaerts, F. Lardon, G. Nijs, M. Lenjou, C. Van Broeckhoven, D. R. Van Bockstaele, and Z. N. Berneman. 2001. Highly efficient gene delivery by mRNA electroporation in human hematopoietic cells: superiority to lipofection and passive pulsing of mRNA and to electroporation of plasmid cDNA for tumor antigen loading of dendritic cells. *Blood 98:49.*
43. Dyall, J., J. B. Latouche, S. Schneil, and M. Sadelain. 2001. Lentivirus-transduced human monocyte-derived dendritic cells efficiently stimulate antigen-specific cytotoxic T lymphocytes. *Blood 97:114.*
44. Araki, K., T. Imaizumi, T. Sekimoto, K. Yoshinobu, J. Yoshimuta, M. Akizuki, K. Miura, M. Araki, and K. Yamamura. 1999. Exchangeable gene trap using the Cre/mutated lox system. *Cell. Mol. Biol. 45:737.*
45. Wakitani, S., K. Takaoka, T. Hattori, N. Miyazawa, T. Iwanaga, S. Takeda, T. K. Watanabe, and A. Tanigami. 2003. Embryonic stem cells injected into the mouse knee joint form teratomas and subsequently destroy the joint. *Rheumatology 42:162.*
46. Wakayama, T., V. Tabar, I. Rodriguez, A. C. Perry, L. Studer, and P. Mombaerts. 2001. Differentiation of embryonic stem cell lines generated from adult somatic cells by nuclear transfer. *Science 292:740.*
47. Hochedlinger, K., and R. Jaenisch. 2002. Monoclonal mice generated by nuclear transfer from mature B and T donor cells. *Nature 415:1035.*
48. Li, F., S. Lu, L. Vida, J. A. Thomson, and G. R. Honig. 2001. Bone morphogenetic protein 4 induces efficient hematopoietic differentiation of rhesus monkey embryonic stem cells in vitro. *Blood 98:335.*
49. Kaufman, D. S., E. T. Hanson, R. L. Lewis, R. Auerbach, and J. A. Thomson. 2001. Hematopoietic colony-forming cells derived from human embryonic stem cells. *Proc. Natl. Acad. Sci. USA 98:10716.*

THE JOURNAL OF BIOLOGICAL CHEMISTRY
Vol. 279, No. 46, Issue of November 12, pp. 48457–48465, 2004
Printed in U.S.A.

B-Raf Contributes to Sustained Extracellular Signal-regulated Kinase Activation Associated with Interleukin-2 Production Stimulated through the T Cell Receptor*

Received for publication, March 19, 2004, and in revised form, August 27, 2004
Published, JBC Papers in Press, August 31, 2004, DOI 10.1074/jbc.M403087200

Hirotake Tsukamoto, Atsushi Irie, and Yasuharu Nishimura‡

From the Department of Immunogenetics, Graduate School of Medical Sciences, Kumamoto University, Honjo 1-1-1, Kumamoto 860-8556, Japan

A T cell receptor (TCR) recognizes and responds to an antigenic peptide in the context of major histocompatibility complex-encoded molecules. This provokes T cells to produce interleukin-2 (IL-2) through extracellular signal-regulated kinase (ERK) activation. We investigated the roles of B-Raf in TCR-mediated IL-2 production coupled with ERK activation in the Jurkat human T cell line. We found that TCR cross-linking could induce up-regulation of both B-Raf and Raf-1 activities, but Raf-1 activity was decreased rapidly. On the other hand, TCR-stimulated kinase activity of B-Raf was sustained. Expression of a dominant-negative mutant of B-Raf abrogated sustained but not transient TCR-mediated MEK/ERK activation. The inhibition of sustained ERK activation by either expression of a dominant-negative B-Raf or treatment with a MEK inhibitor resulted in a decrease of the TCR-stimulated nuclear factor of activated T cells (NFAT) activity and IL-2 production. Collectively, our data provide the first direct evidence that B-Raf is a positive regulator of TCR-mediated sustained ERK activation, which is required for NFAT activation and the full production of IL-2.

T cells recognize self or non-self peptides in the context of major histocompatibility complex (MHC)[1]-encoded molecules via T cell receptors (TCRs), and the signals are then transduced into the nucleus. These signals determine the fate of T cells and induce cytokine production, cytolytic activity, survival, apoptosis, and proliferation (1). Within seconds of MHC-peptide engagement, TCR components initiate phosphorylation cascades that trigger multiple branching signaling pathways. One well studied key switch is the activation signal of extracellular signal-regulated kinase 1/2 (ERK1/2), which is mediated by the small GTP-binding proteins, Ras (2, 3) and Rap1 (4, 5). Current models suggest that TCR stimulation with the agonistic peptide-MHC complex activates the conversion of Ras from the GDP- to GTP-bound form (2, 6). Activated Ras subsequently recruits the serine/threonine kinase Raf-1 to the plasma membrane, resulting in its activation. Activated Raf-1 then activates ERK kinase (MEK), which directly phosphorylates tyrosine and threonine residues (TEY motif) on ERK1/2 to activate them (6). These signals combine to activate multiple transcription factors, including nuclear factor of activated T cells (NFAT), NF-κB, and activating protein-1 (AP-1), all of which contribute toward the production of IL-2 (7–9).

ERK1/2 are involved in a diverse array of cellular functions including cell growth and apoptosis of T cells (10–12). In ERK1-deficient mice, the thymocyte differentiation from $CD4^+CD8^+$ double positive to the $CD4^+/CD8^+$ single positive stage is impaired; thus, ERK activation by TCR ligation plays important roles in T cell development (13). Experiments using pharmacological inhibitors of MEK and dominant negative MEK also provided evidence that ERK1/2 are critical for thymocyte differentiation (11, 14) and for induction of TCR-mediated mitogenic signals and IL-2 production in mature T cells (7, 15). Hence, it is important to understand how the strength and duration of ERK activity is regulated in TCR-mediated activation and fate decisions of T cells.

The functions of ERK signaling are regulated by its upstream elements, in particular by members of the Raf family, in various cell types, and three Raf isoforms, Raf-1, A-Raf, and B-Raf, are expressed in mammalian cells (16, 17). Whereas Raf-1 is ubiquitously expressed, B-Raf shows a more restricted expression pattern (18, 19). Mice deficient in the different Raf isoforms exhibit different developmental defects, suggesting the nonredundant function(s) of each Raf isoform (20). A different phenotype of each Raf-deficient mouse is expected to be due, at least in part, to their distinct expression pattern. It was reported that B-Raf exhibits a much more basal kinase activity and a higher affinity toward MEK than does Raf-1 *in vitro* (21). Despite these differences, the specific function(s) *in vivo*, if any, of each Raf isoform is poorly understood. B-Raf was reported to be one component of the receptor-mediated MEK/ERK activation pathway in fibroblasts, B cell lines, and PC12 cells (21–26). Moreover, B-Raf expression in T cells is controversial; in this study, we detected B-Raf protein in Jurkat cells and primary human T cells, whereas others did not (4).

Although Raf-1 is a well characterized effector molecule for ERK activation in the TCR-mediated signaling cascade and IL-2 production in T cells (27), much less attention has been directed to the roles of B-Raf in T cells. We now report that interaction of B-Raf with MEK and B-Raf activity are induced in a TCR stimulation-dependent manner in Jurkat cells. Our data suggest that MEK/ERK activity are selectively regulated through the Ras/B-Raf signaling pathway and that the sustained B-Raf/MEK/ERK activation is indispensable for the

* This work was supported in part by Grants-in-Aid 12051203, 14370115, and 15510165 from the Ministry of Education, Science, Technology, Sports, and Culture, Japan. The costs of publication of this article were defrayed in part by the payment of page charges. This article must therefore be hereby marked "*advertisement*" in accordance with 18 U.S.C. Section 1734 solely to indicate this fact.

‡ To whom correspondence should be addressed: Dept. of Immunogenetics, Graduate School of Medical Sciences, Kumamoto University, Honjo 1-1-1, Kumamoto 860-8556, Japan. Tel.: 81-96-373-5310; Fax: 81-96-373-5314; E-mail: mxnishim@gpo.kumamoto-u.ac.jp.

[1] The abbreviations used are: MHC, major histocompatibility complex; AP-1, activating protein-1; ERK, extracellular signal-regulated kinase; GST, glutathione *S*-transferase; HA, hemagglutinin; IL-2, interleukin-2; MEK, mitogen-activated protein kinase/ERK kinase; NFAT, nuclear factor of activated T cells; TCR, T cell receptor; GFP, green fluorescent protein.

translocation of NFAT into the nucleus and for the production of IL-2.

EXPERIMENTAL PROCEDURES

Cell Preparations and Reagents—Jurkat cell clone, E6–1 from the American Type Culture Collection, and Jurkat cells expressing simian virus 40 large T antigen (TAg-Jurkat) (28) were maintained in RPMI 1640 medium (RPMI) supplemented with 10% fetal calf serum, 2 mM L-glutamine, and penicillin/streptomycin (100 units/ml and 100 μg/ml, respectively). Jurkat cells stably expressing a wild-type or a dominant negative form of B-Raf were established and maintained in RPMI plus 10% fetal calf serum with 2 mg/ml G418. The human $CD4^+$ T cell clone, YN 5–32 and peripheral blood mononuclear cells were prepared as described (29, 30). For transient and stable transfection, 2×10^7 Jurkat cells were resuspended in 500 μl of cytomix (31) with the appropriate cDNAs. The amount of plasmid DNA was held at 40 μg constant by the addition of the pcDNA3 vector control. Cells were electroporated in 310 V at a capacitance of 960 microfarads. Transfectants were analyzed for CD3 and CD28 expression using flow cytometry (BD Biosciences). Anti-CD3 (clone UCHT-1) antibody, anti-CD28 (clone L923) antibody, and rabbit polyclonal anti-GFP antibody were purchased from Pharmingen. Anti-mouse IgG (Fab-specific) antibody was from Sigma. Mouse monoclonal anti-NFAT1 and anti-NFAT2 antibodies and rabbit polyclonal antibodies specific to Raf-1, B-Raf, MEK-1, c-Fos, and Lamin B were purchased from Santa Cruz Biotechnology, Inc. (Santa Cruz, CA). Polyclonal antibodies specific to MEK, phospho-ERK, phospho-p38, and phospho-MEK and a MEK inhibitor, U0126, were purchased from New England Biolabs (Beverly, MA). Mouse monoclonal anti-hemagglutinin (HA) antibody was from Covance (Berkeley, CA). Cy3-labeled anti-rabbit Ig antibody, horseradish peroxidase-conjugated rabbit anti-mouse IgG, and donkey anti-rabbit IgG were from Amersham Biosciences. Anti-human IL-2 antibodies were from R & D Systems (Minneapolis, MN). Recombinant glutathione *S*-transferase (GST)-MEK was prepared as reported (32).

The pcDNA3 expression vectors with HA-tagged wild-type and dominant negative mutant B-Raf cDNAs were provided by Dr. K. L. Guan (33). The RasN17 expression vector was a gift from Dr. T. Kinashi (5). The luciferase reporter construct for IL-2 promoter and AP-1 binding site were kindly provided by Dr. V. A. Boussiotis (34) and Dr. R. M. Niles (35), respectively. The expression vector for GST-MEK was a gift from Dr. Y. Takai (32). NFAT-green fluorescence protein (GFP) reporter construct, consisting of three tandem NFAT-binding sites followed by a gene encoding GFP, was provided by Dr. T. Saito (36).

Cell Stimulation and Inhibitor Treatment—In experiments for stimulation with soluble anti-CD3 antibody for cross-linking, Jurkat cells were incubated on ice for 20 min and then incubated with anti-CD3 antibody (0.25 μg/ml) for 10 min followed by the addition of anti-mouse IgG antibody (1 μg/ml) for 5 min. After the indicated times of incubation at 37 °C, cells were harvested and lysed with lysis buffer (see below). For the analysis of promoter activity and IL-2 production, Jurkat cells (1×10^6/well) were stimulated with immobilized anti-CD3 and CD28 antibodies (5 and 10 μg/ml, respectively). For experiments with inhibitor treatment, cells were preincubated for 30 min with the MEK inhibitor U0126 or Me_2SO as a control. In the time course analyses of the effect of ERK activation on IL-2 production by the treatment with U0126, medium containing U0126 or Me_2SO was added at the indicated time points.

Western Blotting, Immunoprecipitation, and in Vitro Kinase Assay—After the indicated times of stimulation, the Jurkat cells were recovered and lysed with lysis buffer (1% Nonidet P-40, 150 mM NaCl, 50 mM Tris, pH 7.4, 1 mM EDTA, 0.25% sodium deoxycholate, a protease inhibitor tablet (Roche Applied Science)). SDS-PAGE, Western blotting, and immunoprecipitations from the cell lysates were carried out as described (30). Raf-1 and B-Raf were immunoprecipitated from cell lysates of T cells with the anti-Raf-1 and the anti-B-Raf antibodies, respectively, as described above. The immunoprecipitates were resuspended in 25 mM HEPES (pH 7.5), 10 mM $MgCl_2$, 10 mM β-glycerophosphate, 1 mM dithiothreitol, 10 μCi of [γ-^{32}P]ATP (Amersham Biosciences), and 0.8 μg of recombinant GST-MEK protein. Reaction mixtures were incubated at 32 °C for 20 min, and then the reactions were terminated by adding 5× SDS sample buffer, separated on 7% SDS-PAGE under the reducing condition, transferred to nitrocellulose membrane, and exposed to x-ray film. Relative amounts of MEK or ERK phosphorylation were calculated based on the ratio of the intensities of phospho-MEK or phospho-ERK bands to those of the whole MEK or ERK bands in whole cell lysates at each time point. Signal intensities of the bands were quantified by densitometric analysis using NIH Image 6.2 software. Nuclear extracts were prepared from B-Raf mutant- or mock-transfected TAg Jurkat cells for nuclear translocation analysis of NFAT using nuclear/cytosol fractionation kits (BioVision).

Flow Cytometric Analysis and Cytokine Measurement—For the NFAT-GFP reporter assay, the TAg-Jurkat cells expressing B-Raf AA or mock vector were transfected with NFAT-GFP reporter construct and stimulated for 9 h with immobilized anti-CD3 and anti-CD28 antibodies. The expression of GFP was analyzed with a flow cytometer and CellQuest software (BD Biosciences). For intracellular staining, cells were fixed and permeabilized with IntraPrep (Immunotech, Marseille, France) and then stained with appropriate fluorescence-labeled antibodies. IL-2 concentrations in supernatants of T cell culture after 48 h of stimulation were measured in an enzyme-linked immunosorbent assay using anti-human IL-2 antibodies.

Reverse Transcription-PCR—Total RNA extraction and first-strand cDNA synthesis from T cells were done as described (37). The cDNA was subjected to PCR amplification using a set of primers specific for human *B-Raf*: 5′-ACAACAGTTATTGGAATCTCTGG-3′ and 5′-AAATGCTAAGGTGAAAAACG-3′.

Luciferase Assay—Reporter constructs were transfected into the Jurkat cells expressing wild-type or mutant B-Raf. A β-galactosidase expression plasmid was co-transfected to normalize the variations in transfection efficiency. After 12 h of transfection, cells were harvested and stimulated. Luciferase assay was carried out according to the protocol in the Pica Gene kit (Toyo Ink, Tokyo, Japan). β-Galactosidase expression was assessed using the Luminescent β-galactosidase detection kit II (Clontech) according to the manufacturer's instructions.

RESULTS

Expression of B-Raf Proteins in Both Human and Mouse T Cells—We investigated the expression of B-Raf in human and mouse T cells using Western blotting (Fig. 1*A*). Rat PC12 cells, as a positive control gave a 95-kDa band corresponding to B-Raf (*lane 1*), whereas B-Raf expression was negligible in NIH3T3 cells, as reported (*lane 2*) (38). B-Raf was detected in a human $CD4^+$ T cell clone, YN5–32 (*lane 3*) (29, 30), a human T cell line, Jurkat (*lane 4*), and mouse $CD4^+$ T cells isolated from spleens (*lanes 5*). Furthermore, the expression of human B-Raf mRNA was assessed by reverse transcription-PCR using RNAs isolated from the YN5–32 T cell clone and from Jurkat T cells (data not shown). Intracellular staining and flow cytometric analysis also confirmed the B-Raf expression in human CD3-positive peripheral T cells (Fig. 1*B*) and mouse TCR-β chain-positive splenic T cells (Fig. 1*B*, *b*). Taken together, we conclude that B-Raf is expressed in both human and mouse T cells, allowing us to examine B-Raf functions in TCR-mediated T cell activation.

TCR Ligation Induces Both Raf-1 and B-Raf Activation—Cross-linking of TCRs with soluble anti-CD3 antibody, which mimics the engagement of TCR with the agonistic peptide-MHC complex, induced ERK and MEK phosphorylation within 1 min, reaching a maximal level at ~1–3 min in Jurkat cells (Fig. 2*A*). The ERK/MEK phosphorylations displayed similar kinetics and were prolonged for up to 60 min. Next, we performed *in vitro* kinase assays for Raf-1 and B-Raf to estimate the strength and kinetics of their kinase activities. Consistent with the previous report (27), Raf-1 was activated at 3 min after TCR ligation and became inactive within 20 min (Fig. 2*B*). In contrast to the kinetics of Raf-1 activity, there was slight but detectable B-Raf activity even under the basal condition, and B-Raf showed a pronounced increase of its kinase activity at 3 min after TCR stimulation. B-Raf kinase activity was gradually decreased but did last for up to 60 min (Fig. 2*B*). Raf-1 was inactivated after 20 min of TCR ligation; nevertheless, apparent MEK/ERK activation was still sustained up to 60 min (Fig. 2*A*). Intriguingly, the kinetics of TCR-mediated B-Raf activation rather than that of Raf-1 activation was similar to that of MEK/ERK activation. The addition of co-stimulation with an anti-CD28 antibody treatment slightly enhanced the B-Raf activity over time compared with that stimulated with an anti-CD3 antibody alone (Fig. 2*C*).

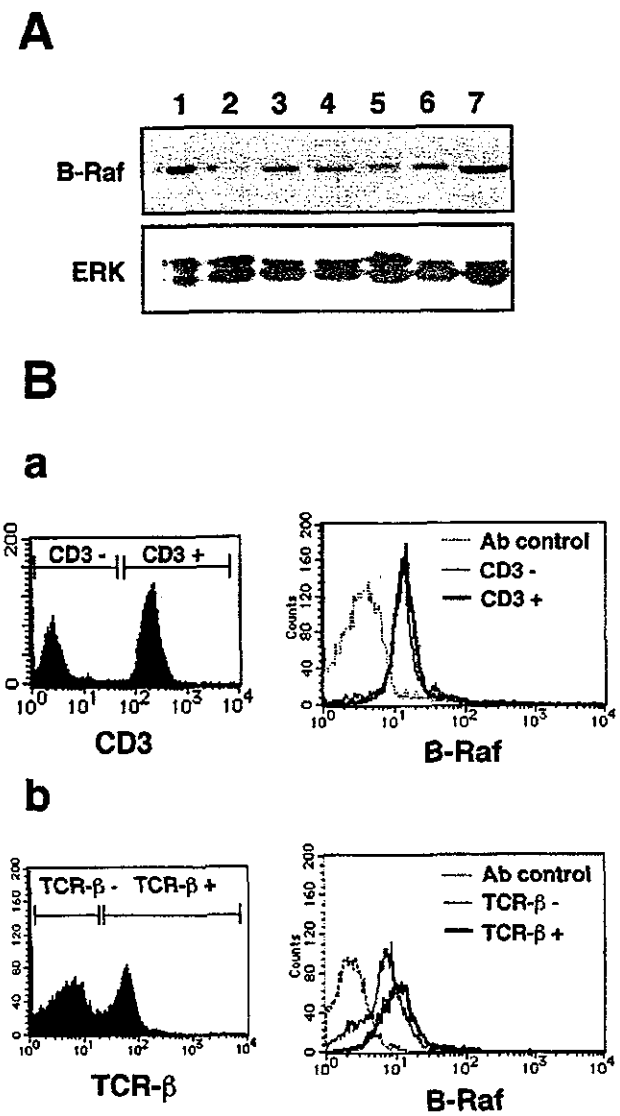

FIG. 1. **B-Raf is expressed in both human and mouse T cells.** *A*, Western blotting analysis using an anti-B-Raf antibody (*top panel*). *Lane 1*, PC12 cells; *lane 2*, NIH3T3 cells; *lane 3*, human $CD4^+$ T cell clone, YN5–32; *lane 4*, Jurkat cells; *lane 5*, mouse $CD4^+$ T cells isolated from spleen; *lane 6*, HeLa cells; *lane 7*, HeLa cells transfected with B-Raf. ERK blotting indicates comparable protein loading (*bottom panel*). *B*, flow cytometric analyses of B-Raf expression. Human peripheral blood mononuclear cells were stained with an anti-CD3 antibody (*a*) and murine spleen cells were stained with anti-mouse TCR-β chain antibody (*b*) (*left panels*). The CD3 or TCR-β chain negative and positive cell populations were gated, and intracellular B-Raf staining was carried out (*right panels*). An irrelevant rabbit polyclonal antibody was used as negative control for staining. *Ab*, antibody.

Physiological association between Raf family kinases and MEK is necessary for MEK/ERK activation (39); hence, we asked if B-Raf can interact with MEK in T cells in response to TCR stimulation using co-immunoprecipitation methods. For this purpose, wild-type B-Raf tagged with HA was expressed in Jurkat cells and was immunoprecipitated with an anti-HA antibody. The specific association between HA-B-Raf and MEK was achieved at a maximal level at 3 min after TCR ligation, and this interaction lasted for up to 60 min with a slight decrease (Fig. 2*D*). The intrinsic interaction between B-Raf and MEK was also evaluated by reciprocal immunoprecipitation experiments using an anti-MEK antibody to detect endogenous B-Raf protein. As shown in Fig. 2*E*, endogenous B-Raf protein was not detected in immunoprecipitates with the anti-MEK antibody in unstimulated Jurkat cells. Consistent with Fig. 2*D*, intrinsic B-Raf-MEK complex formation was strongly induced at 3 min after TCR ligation, and then it decreased gradually but remained above the basal level up to 60 min after TCR stimulation *in vivo* (Fig. 2*E*). The kinetics of B-Raf/MEK interaction paralleled those of B-Raf activation (Fig. 2*B*). These results strongly suggested that B-Raf was involved in MEK/ERK activation stimulated with TCR ligation, especially in the late phase after Raf-1 had become inactive (Fig. 2*B*).

TCR-mediated B-Raf Activation Is Partly Dependent on Ras Activity—Previous studies reported that B-Raf activation in fibroblasts was dependent on Ras activation (40, 41). In other cases, Ras activity was not essential for B-Raf activation in PC12 cells (23, 38). In T cells, to determine whether Ras activity is required for the B-Raf activation, TCR-mediated B-Raf activity was measured in TAg-Jurkat expressing the dominant negative Ras mutant RasN17. The RasN17 interfered with endogenous Ras, Raf-1, and MEK/ERK activation until at least 60 min after TCR stimulation (data not shown) (2). As shown in Fig. 3, TCR engagement resulted in a robust activation of B-Raf after stimulation in mock-transfected Jurkat cells. In contrast, RasN17-transfected cells showed decreased B-Raf activation as compared with that observed in the control cells at 3 min after TCR stimulation (75% reduction). Similar inhibitory effects was observed at any given time points. These results indicated that TCR-mediated B-Raf activation is, at least in part, regulated by Ras activation *in vivo*.

B-Raf Contributes to Sustained MEK/ERK Activation—Within the activation segment of B-Raf, there are two sites, Thr^{598} and Ser^{601}, that can be phosphorylated in response to Ras activation, and the phosphorylation status of these residues is required for the maximal kinase activity of B-Raf (33, 40). Hence, we introduced a dominant negative mutant of B-Raf (B-Raf AA), in which Thr^{598} and Ser^{601} were substituted to Ala (33), into T cells to examine the role of B-Raf in TCR-mediated MEK/ERK activation cascade. As shown in Fig. 4*A*, a Jurkat clone expressing B-Raf AA showed a similar degree of MEK/ERK activation induced by TCR cross-linking with soluble anti-CD3 antibody at 3 min after stimulation in comparison with that of mock-transfected cells. The MEK/ERK activation was effectively sustained for 60 min in the mock transfectants. On the other hand, in the Jurkat clone expressing B-Raf AA, MEK/ERK activation returned to the basal level within 30 min after TCR stimulation, and then it was no longer detected. Densitometric analyses of MEK/ERK activation revealed that the activation kinetic pattern rather than the relative magnitude of MEK/ERK activation was distinct between the mock-transfected clone and the B-Raf AA-expressing clone (Fig. 4*B*). Since TAg-Jurkat cells transiently transfected with B-Raf AA showed an essentially similar response, the possibility that these results were specific for one particular clone (AA2) was excluded (Fig. 4*C*). Moreover, these results were not due to the inhibition of Raf-1 activity by B-Raf AA, because the degree of TCR-mediated Raf-1 activation in B-Raf AA-expressing Jurkat cells was indistinguishable from that of mock-transfected Jurkat cells or cells expressing HA-tagged wild-type B-Raf (Fig. 4*D* and data not shown). In contrast to MEK/ERK activation, no significant differences in phosphorylation of another mitogen-activated protein kinase, p38, were detectable in both mock- and B-Raf AA-transfected TAg-Jurkat cells, suggesting that B-Raf AA did not influence p38 activation (Fig. 4*C*). The data indicate that B-Raf physiologically and specifically regulated prolonged MEK/ERK activation induced by TCR stimulation in Jurkat cells.

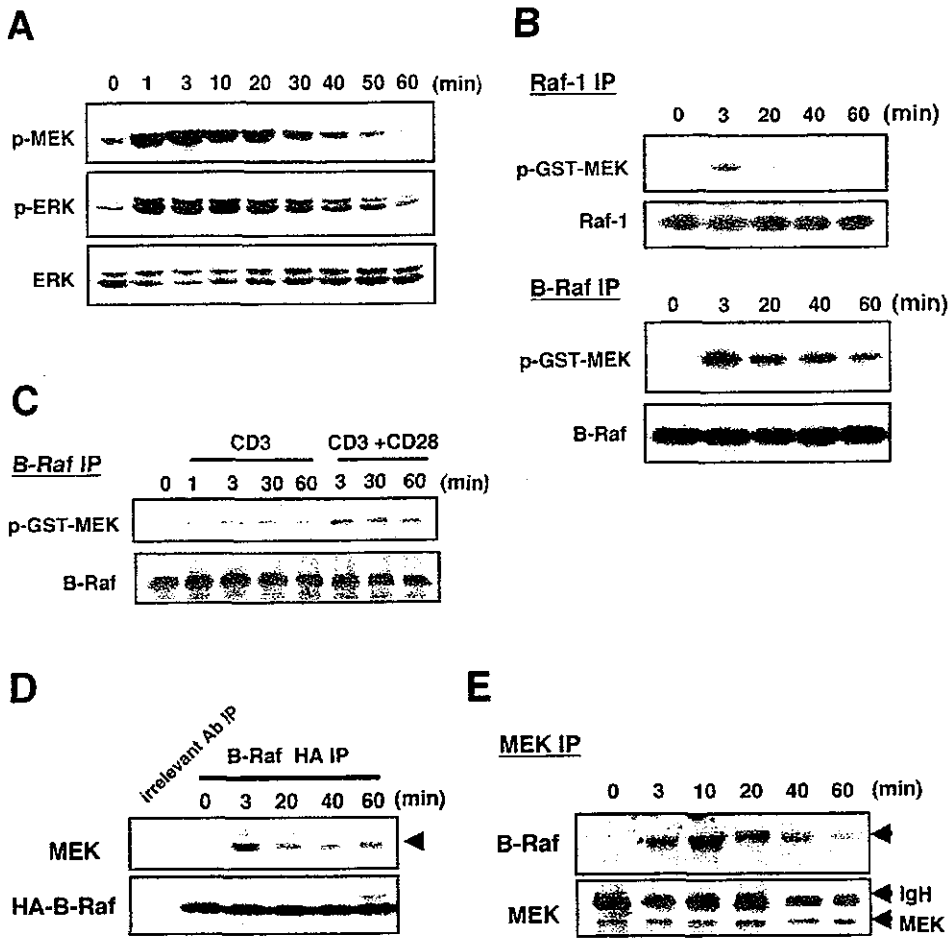

FIG. 2. **B-Raf activation and B-Raf/MEK interaction were induced in a TCR stimulation-dependent manner.** *A*, Jurkat T cells were incubated with or without (0 min) a soluble anti-CD3 antibody together with a second antibody for the indicated times. The cells were subjected to Western blotting with an anti-phospho-MEK-specific antibody (*top panel*) or an anti-phospho-ERK-specific antibody (*middle panel*). Equal protein loading was confirmed by total ERK blotting (*bottom panel*). *B*, *in vitro* kinase assays for Raf-1 and B-Raf isolated from Jurkat cells stimulated with the anti-CD3 antibody for the indicated times. Recombinant GST-MEK was used as a substrate, and incorporated ^{32}P radioactivities were visualized by autoradiography. Equal loading of each Raf protein was confirmed by blotting with either an anti-Raf-1 antibody (*upper bottom panel*) or an anti-B-Raf antibody (*lower bottom panel*). *C*, additive anti-CD28 antibody stimulation enhanced the B-Raf kinase activity. Jurkat cells were stimulated with the anti-CD3 antibody alone or the anti-CD3 together with the anti-CD28 antibodies for the indicated times, and an *in vitro* kinase assay was performed. *D*, TAg-Jurkat cells transiently expressing HA-tagged wild-type B-Raf were stimulated with cross-linking of soluble anti-CD3 antibody for the indicated times. Immunoprecipitates with an anti-HA antibody were blotted with an anti-MEK (*upper panel*) or the anti-HA antibodies (*lower panel*). The immunoprecipitates with irrelevant rabbit IgG in Jurkat cells stimulated for 3 min was used as a negative control. *E*, immunoprecipitates with an anti-MEK antibody from Jurkat cells stimulated with the anti-CD3 antibody for the indicated times were blotted with the anti-B-Raf antibody (*upper panel*). The same membrane was reprobed with the anti-MEK antibody (*lower panel*) to monitor equal protein loading. The data are representative of three reproducible experiments in all analyses. *Ab*, antibody; *IP*, immunoprecipitation.

B-Raf Activation and Subsequently Sustained ERK Activation Is Required for Full IL-2 Production—Since IL-2 production is one of the most critical events of ERK-mediated T cell activation, we first utilized the reporter assay controlled by the IL-2 promoter element to investigate the effect of B-Raf activation on IL-2 promoter activity. Whereas TCR stimulation resulted in induction of luciferase, which reflected the IL-2 promoter activity in wild-type B-Raf-transfected clone (WT30), B-Raf AA significantly attenuated the inducible IL-2 promoter activity (Fig. 5*A*). Indeed, as shown in Fig. 5*B*, TCR stimulation induced a marked increase in IL-2 production in mock-transfected Jurkat cells and in wild-type B-Raf-expressing clones (WT30 and WT34), whereas it was substantially reduced in B-Raf AA-expressing clones (AA2 and AA23).

The data described above clearly indicate that T cells expressing B-Raf AA had defects in sustained ERK activation and subsequent full IL-2 production in comparison with the control cells in response to TCR stimulation. However, whether the sustained ERK activation is directly correlated with the full IL-2 production remained to be solved. To clarify this issue, we investigated the requirement of TCR-mediated sustained ERK activation for the IL-2 production using the pharmacological MEK inhibitor U0126. As shown in Fig. 5*C*, TCR-mediated ERK activation was inhibited by U0126 at the range of 5–10 μM. In addition to ERK activation, IL-2 production provoked by stimulation with immobilized anti-CD3 and CD28 antibodies was markedly blocked by U0126 at the same range of concentrations.

We also examined the effects of B-Raf AA on the magnitude and period of ERK activation stimulated with immobilized anti-CD3 and CD28 antibodies. It must be noted that, as compared with the stimulation by cross-linking of soluble anti-CD3 antibody with the second antibody (Fig. 2*A*), stimulation with immobilized anti-CD3 and -CD28 antibodies resulted in a re-

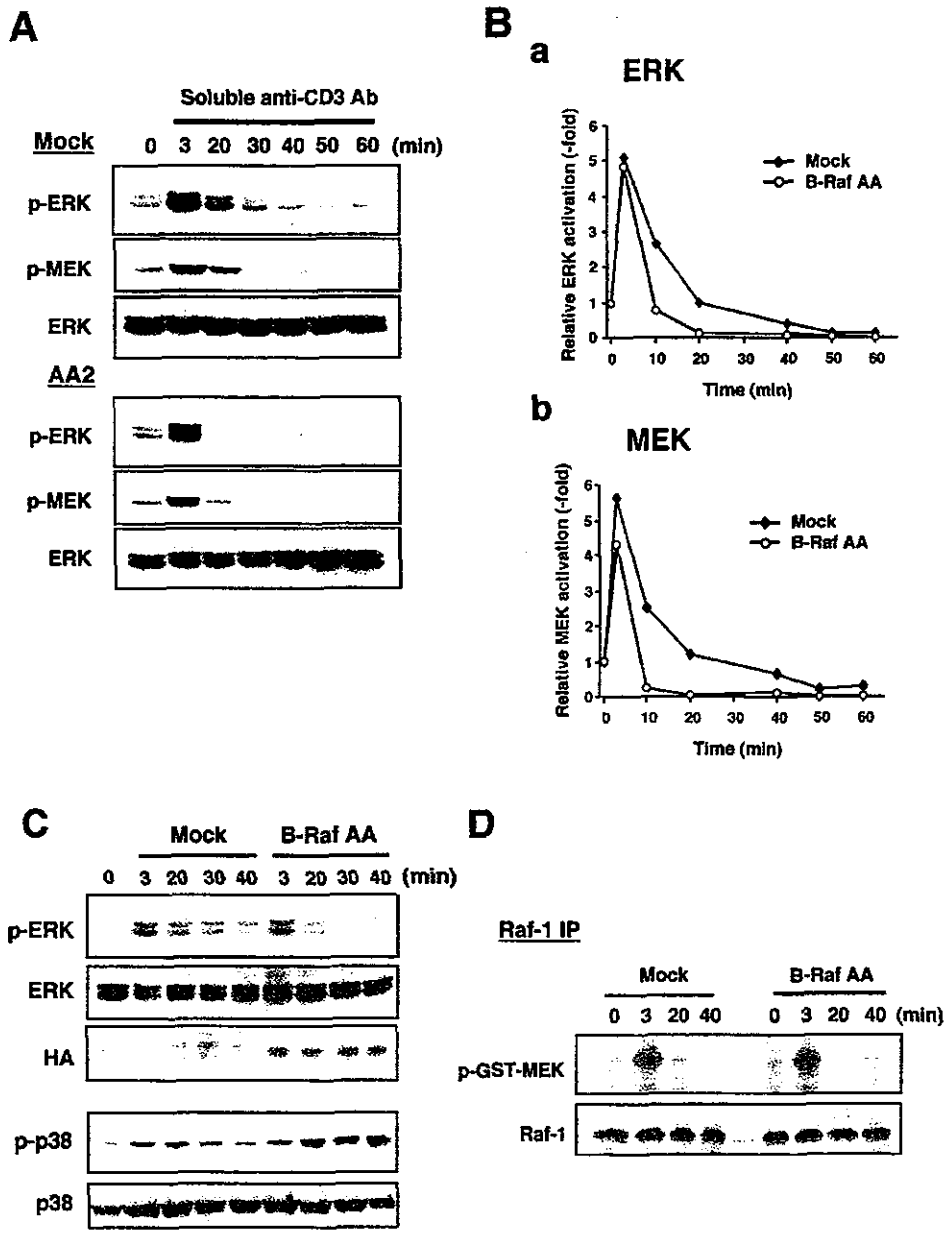

FIG. 4. **Dominant negative B-Raf AA prevented T cells from inducing sustained MEK/ERK activation in response to TCR ligation.** *A*, phosphorylation kinetics of MEK and ERK in Jurkat clones expressing wild-type B-Raf or B-Raf AA (AA2) induced by TCR cross-linking with soluble anti-CD3 antibody. *B*, kinetics of relative amount of phosphorylated ERK (*a*) and MEK (*b*). The relative value of intensity of phosphoprotein bands divided by that of whole ERK bands at each time point observed in mock- or B-Raf AA (AA2)-expressing clone were plotted. The ratio at 0 min was assigned to be 1.0. *C*, Western blotting analyses were done as described in *A* using whole cell lysates from TAg-Jurkat cells transiently transfected with mock or B-Raf AA expression vector and stimulated for the indicated times. Blottings with anti-phospho-ERK, ERK, HA (B-Raf), phospho-p38, or p38 antibodies are shown. *D*, TAg-Jurkat cells transiently transfected with mock vector or with B-Raf AA expression vector were stimulated with TCR cross-linking for the indicated times. *In vitro* kinase assays for Raf-1 were performed using immunoprecipitates from each cell extract with an anti-Raf-1 antibody (*upper panel*). Blotting with anti-Raf-1 antibody indicated equal protein loading (*lower panel*). Each result from three independent experiments was essentially the same, and one is shown.

marker. It is most likely that the defect of NFAT activity in B-Raf AA expressing cells was due to the aberrant nuclear translocation of NFAT1 and NFAT2. Accordingly, these results suggest that TCR-mediated NFAT activation relies on prolonged B-Raf/MEK/ERK activation and that the attenuation of NFAT activation by B-Raf AA reflects the inhibition of TCR-stimulated IL-2 production.

DISCUSSION

Although it is well known that receptor-mediated signals activate the Raf/MEK/ERK cascade, the precise mechanisms of how the TCR signal provokes the cellular response through Raf/MEK/ERK activation remain to be investigated. In mouse models, both Raf-1- and B-Raf-deficient mice resulted in embryonic lethality (20, 45), indicating conclusively that the functions of both Raf isoforms for embryogenesis are not completely overlapping. However, it is poorly understood whether the three Raf isoforms have functional redundancy or if the Raf isoforms play a specific role(s) in T cell activation. Until recently, Raf-1 has been considered to be a major signaling mediator for MEK/ERK activation in TCR-stimulated T cells (27, 46). Our observations provided evidence that the functions of

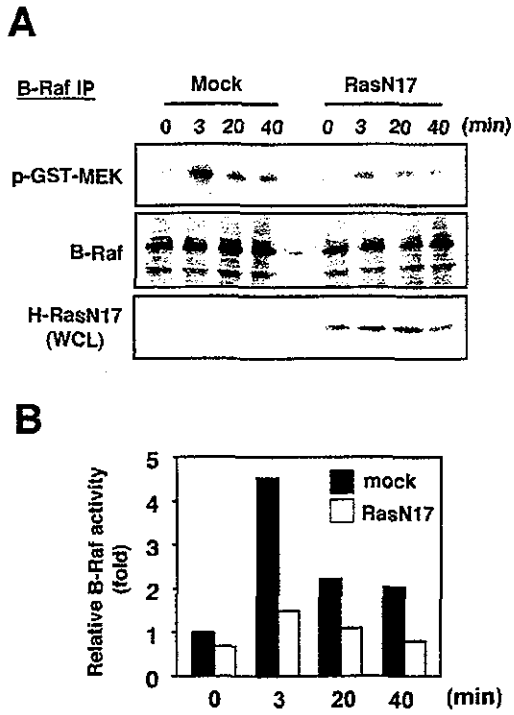

FIG. 3. **Ras-regulated B-Raf activation following TCR stimulation in Jurkat cells.** *A*, TAg-Jurkat cells were transfected with a mock vector or with the RasN17 expression vector, and then these cells were harvested and stimulated with cross-linking of soluble anti-CD3 antibody for the indicated times. Immunoprecipitates from each cell extract with an anti-B-Raf antibody were mixed with the recombinant GST-MEK as a substrate, and *in vitro* kinase reactions for B-Raf were performed. Blotting with an anti-B-Raf antibody showed equal protein loading (*middle panel*). Whole cell lysates (*WCL*) were blotted with anti-H-Ras antibody to monitor the expression of RasN17 (*lower panel*). *B*, the intensity of the GST-MEK phosphorylation by B-Raf immunoprecipitated from mock-transfected (*black bar*) or RasN17-transfected cells (*white bar*) was quantified by densitometric analysis. The relative B-Raf activity at 0 min in mock-transfected cells was assigned to be 1.0. Essentially similar results were obtained in three independent experiments. *IP*, immunoprecipitation.

tardation of ERK activation and extended ERK activation in mock-transfected cells (Fig. 5*D*). Such temporal differences in ERK activation have been reported, and the authors suggested that this phenomenon was due to the difference in TCR occupancy (42). As shown in Fig. 5*D*, in mock-transfected cells, TCR stimulation induced an accumulation of active ERK within 0.5 h, and this lasted for 6 h, whereas the sustained ERK activation over 2 or 3 h was impaired in cells expressing B-Raf AA. The data also confirmed that B-Raf was required for sustained ERK activation. Based on the results of Fig. 5*C*, 5 μM U0126 was used to determine whether the sustained ERK activation that can be suppressed by B-Raf AA, as shown in Fig. 5*D*, was required for the maximal IL-2 production. Continuous treatment of T cells with U0126 over the period of TCR stimulation abolished IL-2 production (Fig. 5*E*). Interestingly, the addition of U0126 after 2 or 4 h of TCR stimulation also reduced IL-2 production to a degree comparable with that of cells treated with U0126 from the beginning of stimulation, although the intense ERK activation was induced for up to 2 h after stimulation. The same condition in which B-Raf AA inhibited the sustained ERK activation can be reproduced by treatment of Jurkat cells with U0126 after 2 or 4 h of TCR stimulation. Therefore, not only the intense ERK activation in the early phase but also the sustained ERK activation in the late phase was necessary for maximal IL-2 production. Concomitantly, these results suggested that the defect of IL-2 production in Jurkat cells expressing B-Raf AA was due to the lack of potential to maintain the TCR-mediated sustained ERK activation although the transient ERK activation was intact.

AP-1 Activation Induced by TCR Ligation Is Not Impaired in Jurkat Cells Expressing B-Raf AA—To define more precisely the biochemical mechanisms underlying the relationship between B-Raf-dependent ERK activation and IL-2 production, we first investigated the TCR-mediated c-Fos induction, one of the downstream targets of ERK (43). As shown in Fig. 6*A*, the expression of c-Fos was induced within 1 h, and its phosphorylation judged by electrophoretic mobility shift was potentiated by TCR stimulation in cells expressing wild-type B-Raf. There was no significant difference in c-Fos induction between Jurkat clones expressing wild-type B-Raf and B-Raf AA up to 3 h (Fig. 6*A*). Next, to examine whether B-Raf contributed to AP-1 activation, we performed a luciferase assay. Consistent with c-Fos induction, the AP-1 promoter activity in response to TCR stimulation in the Jurkat clone expressing B-Raf AA (AA2) was comparable as compared with that of the control clone (WT30) (Fig. 6*B*). Thereby, TCR-mediated c-Fos induction and AP-1 activation seemed to be less dependent on B-Raf.

B-Raf Activity Is Important for TCR-mediated NFAT Activation—The IL-2 production is regulated by nuclear translocation and activation of the NFAT transcription factor cooperating with the AP-1 components c-Fos and c-Jun (7–9). Thus, NFAT-dependent transcriptional events in T cells require the simultaneous activation of multiple Ras effectors such as the ERK and c-Jun N-terminal kinase pathways (44). We analyzed whether TCR-mediated B-Raf activity would influence NFAT activation, using an NFAT-GFP reporter. GFP expression, which is regulated by a promoter corresponding to the NFAT binding site, is increased in a TCR stimulation-dependent manner in mock-transfected cells (Fig. 7*A*, *a*). Comparable transfection efficiency was monitored by co-transfection of a DsRed expression vector (data not shown). In contrast, GFP expression was significantly suppressed in B-Raf AA-expressing cells, suggesting that B-Raf activity is important for the regulation of TCR-mediated NFAT activity. Given that B-Raf regulated TCR-mediated MEK/ERK activation in late phase, there is a possibility that B-Raf activation couples NFAT activation to MEK/ERK activation. For confirmation, we analyzed whether the inhibition of ERK activity in the late phase blocks NFAT reporter activity. As expected, the TCR stimulation-induced GFP expression was reduced by pretreatment with U0126 (Fig. 7*A*, *b*). Furthermore, similar to IL-2 production, the inhibition of NFAT reporter activity was also observed in the presence of U0126 after 2 h of TCR stimulation, although this suppression was less effective than that observed in simultaneous U0126 treatment at the beginning of the TCR stimulation. These results suggested that not only transient but also sustained ERK activation was necessary for the TCR-mediated NFAT activation.

Upon TCR stimulation, NFAT proteins are dephosphorylated by calcineurin, translocate into the nucleus, and then bind to cognate DNA elements (9). Finally, to dissect the mechanism responsible for the B-Raf mediated induction of NFAT activity, we evaluated the nuclear translocation of NFAT protein induced by TCR stimulation. As shown in Fig. 7*B*, the stimulation of mock-transfected Jurkat cells with TCR ligation drove the translocation of NFAT1 and NFAT2 into nucleus at 3 and 5 h of TCR stimulation. In contrast, the substantial nuclear translocation of NFAT1 and NFAT2 could not be observed in B-Raf AA-expressing Jurkat cells under either nonstimulated or TCR-stimulated conditions. Equal loading of nuclear protein in both cells was estimated by blotting of Lamin B as a nuclear

functional redundancy between Raf-1 and B-Raf in early phase. The idea was supported by our observations; the B-Raf AA did not grossly perturb ERK activation when Raf-1 was active in 3–20 min after TCR stimulation (Figs. 2 and 4), suggesting that Raf-1 activity is sufficient to induce ERK activation in the early phase. On the other hand, ERK activation in the late phase (~20 min) was abrogated by B-Raf AA, because the kinase activity of Raf-1 declined, and Raf-1 could no longer compensate for B-Raf activity. Consequently, although we could not exclude the possibility that Raf-1 activity in early phase modulates the TCR-mediated B-Raf activation, our observations led to the model that Raf-1 activity is responsible and sufficient for the early phase MEK/ERK activation, whereas B-Raf activity is essential for the late phase MEK/ERK activation in TCR-stimulated T cells.

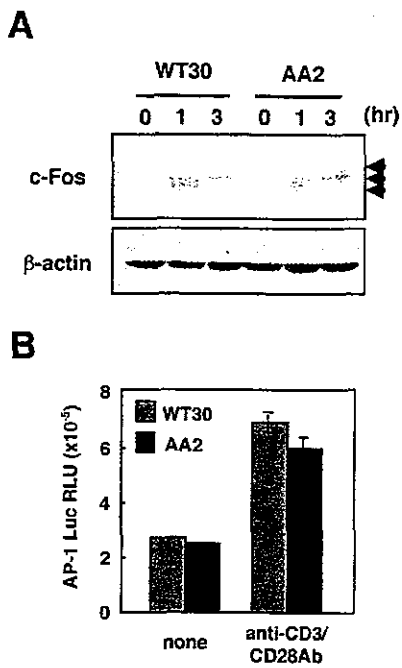

FIG. 6. **B-Raf activity does not influence c-Fos induction and AP-1 activation.** *A*, Western blotting analysis using an anti-c-Fos antibody (*upper panel*). Jurkat clones expressing wild-type B-Raf (WT30) or B-Raf AA (AA2) were stimulated with immobilized anti-CD3 antibody for the indicated times. Blotting with an anti-β-actin antibody indicated equal loading of proteins (*lower panel*). The *arrowheads* indicate the phosphorylated forms of c-Fos. *B*, luciferase assay for AP-1 promoter activity. Jurkat clones expressing wild-type B-Raf (WT30) or B-Raf AA (AA2) together with an AP-1-luciferase construct were stimulated with immobilized anti-CD3 and anti-CD28 antibodies for 8 h followed by a 12-h culture. Each luciferase activity was measured and normalized by the co-transfected β-galactosidase activity. *RLU*, relative luciferase unit. The data are representative of three independent and reproducible experiments. *Ab*, antibody.

ERK activation is critical for the precise outcome of T cell activation, including IL-2 production (7, 15). The marked decrease in IL-2 production in T cells by the expression of B-Raf AA and by the inhibition of the late phase ERK activation using U0126 leads to the conclusion that ERK activation in the late phase regulated by B-Raf was critical for the full IL-2 production in response to TCR stimulation. In view of no defect of TCR-mediated c-Fos induction and AP-1 activation in Jurkat cells expressing B-Raf AA, it was indicated that these events were less dependent on B-Raf activity. In contrast to AP-1 activation, we found that B-Raf AA inhibited TCR-mediated nuclear translocation of NFAT and NFAT-mediated reporter activation (Figs. 6 and 7). The correlation between B-Raf and these transcriptional factors was also noted by Brummer *et al.* (24), who reported that in B-Raf null chicken B cells, B cell receptor-mediated ERK activation was eliminated in only late phase, whereas c-Fos induction was not abrogated. On the contrary, the loss of B-Raf expression resulted in significant defects in the B cell receptor-mediated activation of NFAT transcription factor, suggesting that NFAT activation is regulated by B-Raf in chicken B cells. The selective role of TCR-mediated B-Raf activation in NFAT regulation was consistent with that observed in B cells, and their regulatory mechanisms may be conserved between immunoreceptor-mediated activation in both B and T cells. These results suggest that NFAT-responsible transcriptions and subsequent IL-2 production were dependent on B-Raf and that Raf-1-induced ERK activation in the early phase is not sufficient to provoke these immunoreceptor-mediated activations.

It was expected that the inhibitory effect of B-Raf AA on NFAT activation was due to a defect in sustained ERK activation mediated by B-Raf, because the treatment of Jurkat cells with MEK inhibitor also reduced the NFAT activation. Evi-

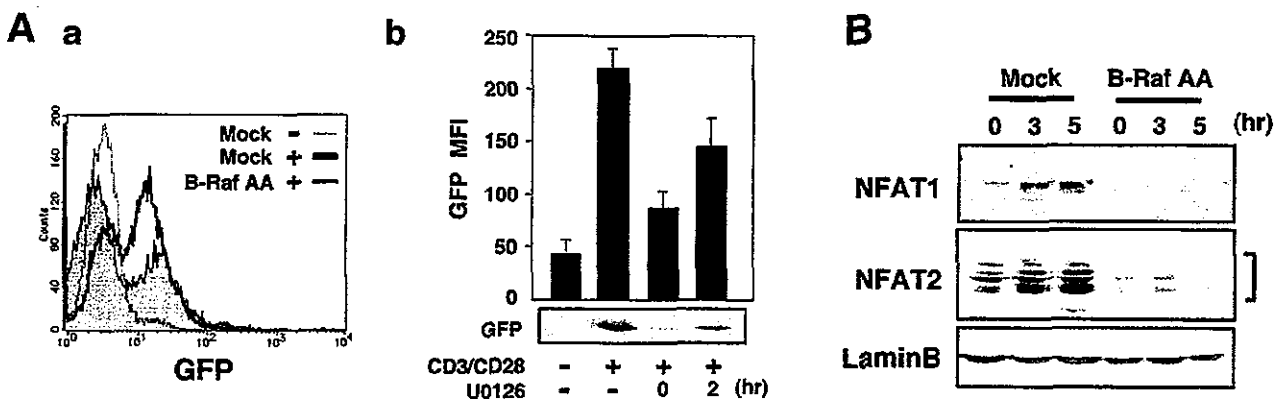

FIG. 7. **B-Raf activity is required for NFAT activation.** *A*, *a*, TAg-Jurkat cells co-transfected with the NFAT-GFP reporter construct and mock or B-Raf AA expression vector were stimulated with (+) or without (−) immobilized anti-CD3 and anti-CD28 antibodies for 9 h. A representative flow cytometric profile for GFP expression is shown. *b*, NFAT-GFP-transfected Jurkat cells were stimulated, and then GFP expression was examined by blotting with anti-GFP antibody (*lower panel*) and flow cytometry (*upper panel*). The *diagram* represents the average of GFP mean fluorescence intensity (*MFI*) obtained from three independent experiments. U0126 (5 μM) was added to the culture at 0 or 2 h after TCR stimulation. *B*, nuclear extracts were isolated from mock- or B-Raf AA-transfected cells stimulated with or without immobilized anti-CD3 and anti-CD28 antibodies for indicated times. Then, the nuclear fractions were separated by SDS-PAGE, and the translocations into nucleus of NFAT1 and NFAT2 were analyzed by Western blotting. Blotting with anti-Lamin B antibody indicated the appropriate nuclear fractionation and protein loading. Essentially similar results were obtained in three independent experiments.